ORNL/SPR-2023/3058

Rogers Quarry Special Studies Report 2023

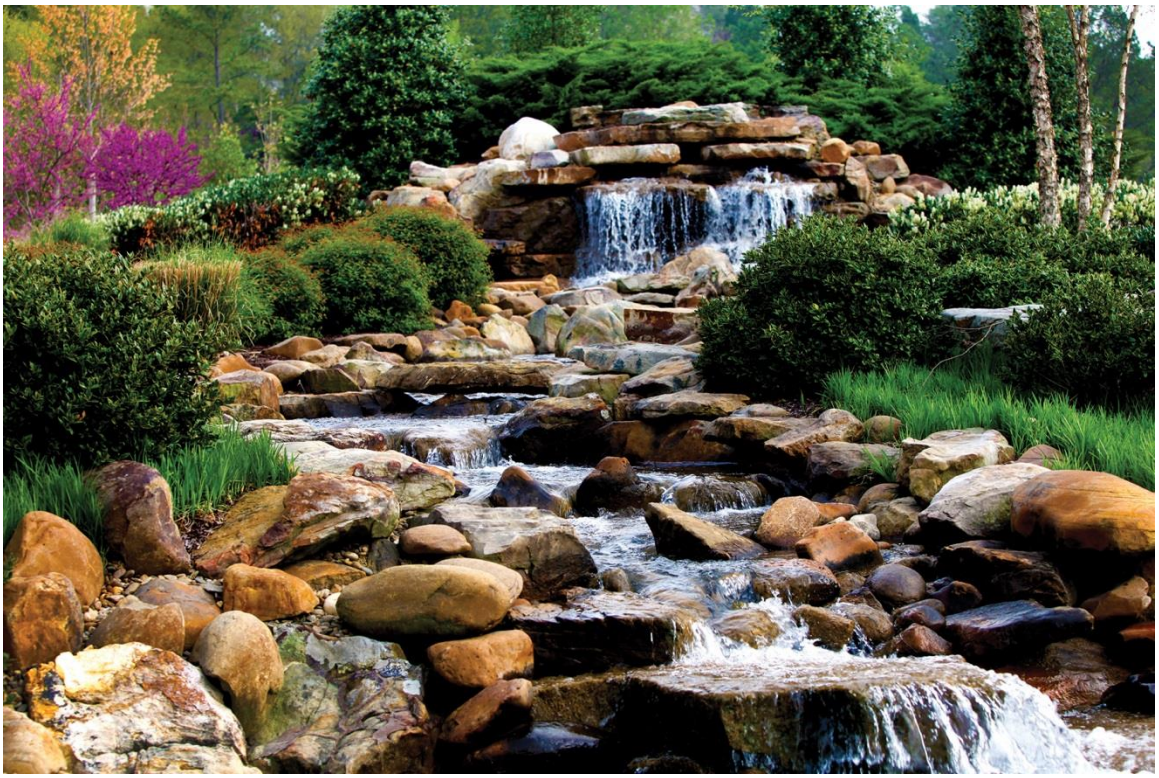

S. C. Brooks
T. J. Mathews
R. T. Jett
P. G. Matson
M. W. Jones
A. M. Fortner
K. A. Lowe
N. J. Jones

September 2023

OAK RIDGE National Laboratory

ORNL IS MANAGED BY UT-BATTELLE LLC FOR THE US DEPARTMENT OF ENERGY

ORNL/SPR-2023/3058

Environmental Sciences Division

ROGERS QUARRY SPECIAL STUDIES REPORT 2023

S. C. Brooks
T. J. Mathews
R. T. Jett
P. G. Matson
M. W. Jones
A. M. Fortner
K. A. Lowe
N. J. Jones

September 2023

Prepared by
OAK RIDGE NATIONAL LABORATORY
Oak Ridge, TN 37831-6283
managed by
UT-BATTELLE, LLC
for the
US DEPARTMENT OF ENERGY
under contract DE-AC05-00OR22725

CONTENTS

LIST OF FIGURES

LIST OF TABLES

ABBREVIATIONS

AIC_c	corrected Akaike information criterion
AWQC	ambient water quality criteria
DO	dissolved oxygen
EFPC	East Fork Poplar Creek
EPA	US Environmental Protection Agency
FCAP	Y-12 National Security Complex Filled Coal Ash Pond
Hg_D	dissolved Hg
Hg_T	total Hg
ICP-MS	inductively coupled plasma–mass spectrometry
MB	McCoy Branch
MCK	McCoy Branch kilometer
MeHg	methylmercury
$MeHg_D$	dissolved MeHg
$MeHg_T$	total MeHg
PEC	probable effect concentration
PETG	polyethylene terephthalate
RQ	Rogers Quarry
TSS	total suspended solids

1. BACKGROUND

Rogers Quarry (RQ) has a history of elevated Se concentrations in water and fish caused by inputs from the Y-12 National Security Complex Filled Coal Ash Pond (FCAP). Selenium is acutely toxic at high concentrations, and chronic toxicity occurs at low aqueous concentrations because Se bioaccumulates in fish tissues. The US Environmental Protection Agency (EPA) recently developed water quality criteria for Se that include fish tissue as well as aqueous Se concentrations. The water column concentration criterion is 1.5 μg L^{-1} for lentic ecosystems and 3.1 μg L^{-1} for lotic ecosystems. The fish tissue criteria include both an egg/ovary concentration (15.1 μg/g dry weight) and a concentration for whole-body (8.5 μg/g dry weight) or fish muscle (11.3 μg/g dry weight). The egg/ovary criterion supersedes the fillet and aqueous concentrations if measured because Se toxicity manifests via reproductive effects in birds and fish. It is maternally transferred through eggs, leading to teratogenicity (i.e., deformities, developmental effects) in young fish.

RQ has been routinely sampled for resident largemouth bass (*Micropterus salmoides*) since 1990. In the 1990s, deformities were observed in largemouth bass collected in the quarry, and Se concentrations in fillets were above the new fillet criterion. In response, a wetland area was established just downstream of the FCAP to entrain ash particles. This wetland area successfully reduced inputs of ash and Se to the quarry for the next decade, but a spike in fillet Se concentrations was observed in 2008 and 2009. These elevated concentrations would have exceeded the 2016 fillet criterion, but no obvious effects were observed in fish at that time. In 2016, one-third of the largemouth bass specimens retained for bioaccumulation exhibited abnormalities consistent with Se exposure (e.g., severe emaciation, spinal deformities), although tissue concentrations were below the Se criterion. Two of the many fish that were collected and released to the quarry had documented abnormalities consistent with Se toxicity.

The presence of abnormalities in wild fish populations reflects the combined effects of all stressors to which fish are exposed and provides a readily measurable index of fish health and habitat quality. A high prevalence of abnormalities suggests that fish populations are under stress, and long-term changes in prevalence suggest changes in stressor exposure. Because of the relatively small sample size collected for the bioaccumulation studies, it was unclear whether the deformities observed in RQ fish were representative of the population as a whole or whether the incidence was greater than would be expected in a natural population. Since 2016, in addition to bioaccumulation studies, fish population and fish health surveys have been conducted in RQ to track incidences of any abnormalities.

Historical bioaccumulation data suggest that Se is likely the primary contaminant of concern in RQ, but more recent sampling shows that aqueous arsenic (As) concentrations in upper McCoy Branch (MB) have been elevated and could also affect resident biota. The methods and results from a water and fish field collection campaign in May 2023 are presented in this report. The study evaluated the extent of abnormalities in the RQ fish population and examined potential causal factors. More recently, Se concentrations in fish collected from upper MB were found to be above the tissue criterion for Se for whole body fish. In FY 2019, actions were taken to deepen the constructed wetland just downstream of the FCAP to increase its ability to remove coal ash particulates from the water column before water enters MB. Sampling was conducted throughout MB in FY 2020–2023 to evaluate the effectiveness of the actions taken in the FCAP wetland and to measure Se concentrations in biota throughout the watershed.

2. METHODS

2.1 WATER QUALITY AND SOLIDS SAMPLING AND ANALYSIS

RQ and MB were sampled on May 10 and 11, 2023, respectively. These sampling events followed previous campaigns from 2017 to 2022. During sampling, several water quality parameters were measured in the field, and surface water and solid phase samples were collected, processed, and preserved in the field for subsequent laboratory analysis (Table 1). Additionally, a vertical profile of the field parameters was collected within RQ, and water samples for laboratory analysis were collected from three depths (at the surface, at approximately the depth of the thermocline, and near the bottom; Table 2). Dedicated samples for Se and As analysis were collected and submitted to Brooks Applied Labs for analysis by EPA Method 1638 (EPA 1996), modified with closed-vessel bomb digestion for aqueous samples. Solid phases collected for sampling included creek sediments, bottom sediments from RQ, creek bank soils, discrete coal ash layers (2017 and 2020 sampling campaigns) in exposed creek banks, and benthic biofilms (hereinafter referred to as *biofilms*) scraped from rocks and substrates on the creek bed. Biofilm samples include algae, bacteria, fungi, microinvertebrates, and fine organic and inorganic particulate matter and are taken as an indicator of what might be ingested by scrapers and grazers.

Table 1. Parameters measured on samples collected from McCoy Branch and Rogers Quarry

Field measures	Laboratory measures
Temperature	Dissolved[a] and total Hg in water
pH	Dissolved[a] and total MeHg in water
Dissolved O_2	Total suspended solids in water
Turbidity[b]	As and Se
Specific conductance	Anions (Cl^-, NO_3^-, SO_4^{2-}, PO_4^{3-}) [a]
Depth profile in quarry	Cations (major and trace metals)[a]
	Dissolved[a] Fe(II) and S(II)
	Nonpurgeable dissolved[a] organic carbon
	Ultraviolet–visible spectroscopy absorbance characteristics and dissolved organic carbon character
	Total elemental composition of solid phases, including total Hg and total MeHg

[a]Passes a 0.2 μm pore size filter.
[b]Rogers Quarry only.

Bulk 500 mL water samples were collected in new glycol-modified polyethylene terephthalate (PETG) bottles that were first triple-rinsed with water before sample collection took place. A separate sample for total suspended solids (TSS) was collected in a 2 L high-density polyethylene bottle. Concurrent with water sampling, ambient water conditions (temperature, specific conductance, pH, and dissolved oxygen [DO]) were measured using an In-Situ AquaTroll 9500 (In-Situ Inc., Fort Collins, Colorado). Fine-grained sediments and bank soils were collected into new 50 mL conical centrifuge tubes. Sediments were placed on ice until brought to the laboratory, where they were subsequently lyophilized and stored until analysis.

Water samples were processed as soon as possible in the field and placed on ice until brought to the lab for storage until analysis. An unfiltered aliquot of each sample was retained for quantification of total Hg (Hg_T) and total MeHg ($MeHg_T$). The remaining sample was filtered through a 0.2 μm pore size

polyethersulfone filter using an analytical filter unit to analyze dissolved Hg (Hg_D), dissolved MeHg ($MeHg_D$), dissolved organic carbon, ultraviolet-visible spectroscopy absorption, anions, and metals. Samples collected for total suspended solids analysis were filtered in the lab through a tared Whatman glass fiber filter with 0.7 μm particle retention. Unfiltered and filtered Hg and MeHg samples were preserved to 0.5% volume/volume (v/v) trace metal–grade HCl in PETG bottles. Dissolved organic carbon samples were preserved to 0.1% (v/v) trace metal–grade HCl in amber glass bottles. Samples for metals analysis were acidified to 0.5% (v/v) with trace metal–grade HNO_3 in clear glass bottles. Samples for anion analysis were kept in clear glass bottles, and samples for ultraviolet-visible spectroscopy analysis were kept in amber glass bottles. All samples were stored in the dark at 4°C until analysis. Solids were freeze-dried and held at 4°C until analysis.

Water and solids samples for Hg and MeHg analysis were submitted to Brooks Applied Labs (Seattle, Washington), where the samples were analyzed by EPA Methods 1631 (for Hg analysis samples) and 1630 (for MeHg analysis samples). Water samples for total and dissolved Se and As analysis were also submitted to Brooks Applied Labs and were processed by closed vessel bomb digestion and analyzed using triple quadrupole inductively coupled plasma–mass spectrometry (ICP-MS) following a modified EPA Method 1638. Water and solids samples for total elemental analysis were submitted to Actlabs (Ontario, Canada), where water samples were analyzed by ICP-MS, and solids samples were analyzed by aqua regia digest followed by ICP-MS.

Dissolved organic carbon concentrations were measured using high-temperature Pt-catalyzed combustion followed by infrared detection of CO_2 (Shimadzu TOC-5000A or Shimadzu TOC-L). Ultraviolet-visible spectra were collected at 1 nm intervals and 0.5 s exposure time from 190 to 1,100 nm wavelengths with an HP 8453 spectrophotometer using a 1 cm path length quartz cuvette. Dissolved anions (Cl^-, NO_3^-, SO_4^{2-}, and PO_4^{3-}) were analyzed by ion chromatography (Dionex DX-120, Sunnyville, California).

Table 2. Sampling summary in the McCoy Branch (MB)/Rogers Quarry (RQ) watershed

Date	Days since last significant rain[a]	Water body	Sites
April 25, 2017	2	RQ	Depth profile
August 3, 2017	6	RQ	Depth profile
August 3, 2017	6	MB	MCK[b] 2.05, 1.90, 1.75[c], 1.60
April 30, 2018	6	RQ	Depth profile
May 7, 2018	13	Lamberts Quarry	Depth profile
May 16, 2018	22	Harriman Quarry	Depth profile
June 5, 2018	5	University of Tennessee Arboretum Quarry	Depth profile
April 24, 2019	5	RQ	Depth profile
July 9, 2019	15	RQ	Depth profile
July 9, 2019	15	MB	MCK[b] 2.05, 2.0, 1.9, 1.75[c], 1.6
April 22, 2020	2	RQ	Depth profile
May 12, 2020	17	MB	FCAP[d], MCK[b] 2.05, 2.0, 1.9, 1.75[c], 1.6
April 22, 2021	22	RQ	Depth profile
May 19, 2021	10	MB	FCAP[d], MCK[b] 2.05, 2.0, 1.9, 1.6
May 18, 2022	12	RQ	Depth profile
June 6, 2022	4	MB	FCAP[d], MCK[b] 2.05, 2.0, 1.9, 1.6
May 10, 2023	2	RQ	Depth profile
May 11, 2023	3	MB	FCAP[d], MCK[b] 2.05, 2.0, 1.9, 1.6

[a]Number of days since last daily rainfall total ≥0.5 in. as measured at National Weather Service station KOQT in Oak Ridge, Tennessee.
[b]MCK = MB kilometer, measured upstream from mouth.
[c]MCK 1.75 = surface water sample in RQ.
[d]FCAP = water sampled on Y-12 National Security Complex Filled Coal Ash Pond.

2.2 BIOTA SAMPLING

2.2.1 Bioaccumulation Study in the MB and RQ Watershed

Contaminant bioaccumulation in fish was assessed at several locations along MB and RQ (Figure 1). Sampling in 2023 followed campaigns from previous years. In addition to conducting longitudinal sampling of fish for metals analysis in upper and lower MB and extending into RQ and the MB embayment of the Melton Hill Reservoir (Figure 1), caged Asiatic clams (*Corbicula fluminea*) were used as bioindicators of contaminant sources in MB and RQ. Because clams are sedentary filter feeders, they accumulate contaminants that are present in the water and in suspended particles at a given site. Clams are useful indicators of the bioavailable (and therefore potentially toxic) portion of contaminants that enter the environment at a given location, and they provide spatial resolution of contamination on a finer scale than is possible with fish bioaccumulation studies. Caged clams have been used for more than 20 years to evaluate the importance of storm drains and other inputs of contaminants across the Oak Ridge Reservation and may be of particular use in tracking exposure to coal ash particulates in the MB and RQ watershed.

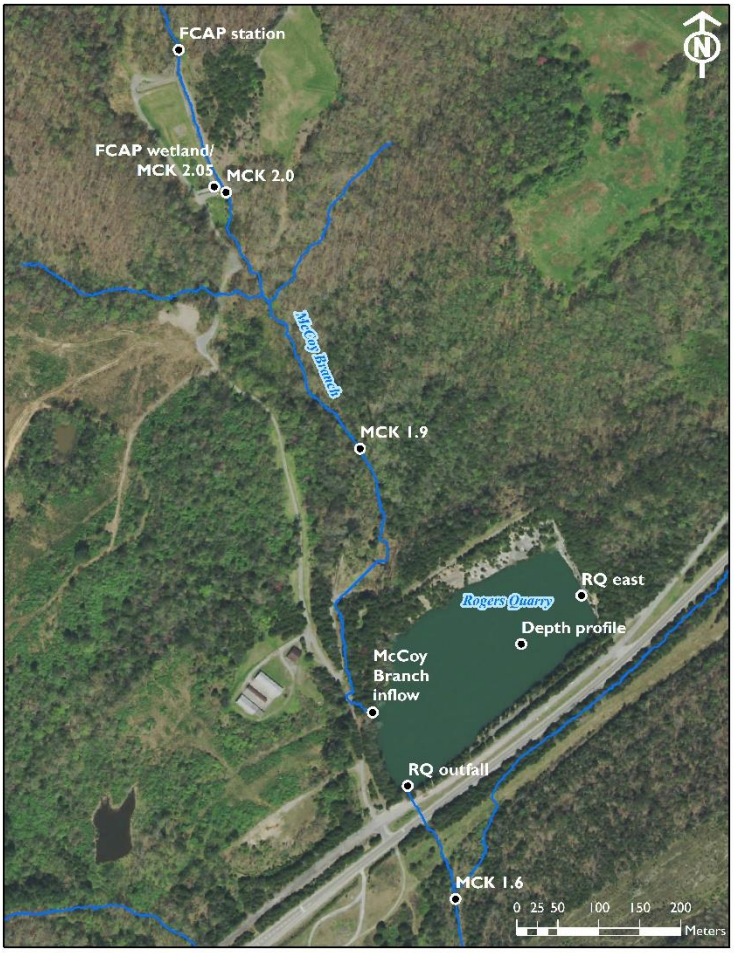

Figure 1. Sampling sites for McCoy Branch (MB) and Rogers Quarry (RQ).
Samples were collected in RQ and at MB kilometers (MCKs) 1.6, 1.9, and 2.0.

To the fullest extent possible, fish collections were coordinated with other activities (e.g., abiotic sampling and Biological Monitoring and Abatement Program sampling already in progress). Fish sampling in MB was conducted by backpack electrofishing, whereas RQ was sampled by launching two small boats with battery-powered motors. Rod and reel angling occurred for 3.0 h, with all fish kept in holding nets.

Forage fish were collected from MB. Blacknose dace (*Rhinichthys obtusus*) were collected at all MB sites, and bluntnose minnow (*Pimephales notatus*) were collected only from lower MB (MB kilometer [MCK] 1.6). Largemouth bass were collected from RQ. Forage fish were homogenized and analyzed as whole-body composites to assess the ecological risk; largemouth bass tissue analysis included ovaries to evaluate risks to ecological health and fillets to evaluate risks to human health. As in previous years, six largemouth bass of various sizes were processed for bioaccumulation analysis. An effort was made to identify female largemouth bass so that ovaries could be collected. Fillets and ovaries from six largemouth bass were analyzed for Hg and metals. Clams were collected from an uncontaminated reference site (Little Sewee Creek in Sweetwater, Meigs County, Tennessee) and were divided into groups of 10 clams of equal mass. Clams were then placed in baskets to be deployed at strategic locations in MB and RQ for a 4-week exposure period (April 12 to May 10, 2023). Locations for clam deployment included the same sites monitored for fish (MCKs 2.0, 1.9, and 1.6), as well as within the FCAP wetland and at the inlet and outlet of MB in RQ, both at the surface and just above the thermocline (approximately

8 m in depth). Clam baskets were also placed at the surface and at depth on the east side of RQ to assess the homogeneity of contaminant concentrations within the quarry. Two clam baskets were placed at each site with 10 clams in each basket. After the exposure period, the soft tissues of the clams from each cage were homogenized, and aliquots were taken for metals analysis.

2.2.2 Fish Population Abundance Estimation and Community Survey

To quantify the prevalence of abnormalities and to determine the likelihood that these deformities are caused by exposure to Se or other stressors, a reliable estimate of the population and survival of largemouth bass in RQ is critical. A mark-recapture survey has been ongoing in RQ since 2017. Mark-recapture surveys are commonly used for estimating fish population abundance. Fish for mark-recapture estimation were collected by angling, marked using passive integrated transponder tags, and released for later recapture sampling. Fish characteristics such as length, weight, and condition at the time of capture were also noted.

A POPAN model (Schwarz and Arnason 1996) was used to estimate largemouth bass population size using mark-recapture data collected between April 2017 and April 2023. This robust open population model was developed to parameterize the Jolly-Seber model in terms of apparent survival (ϕ), capture probability (p), superpopulation size (all individuals that comprised a population during the study period), and the probability of entry into the population (*pent*). This model requires an initial marking period plus two mark-recapture periods. Therefore, for this study, 3 years of mark-recapture work were required for an initial survival estimate. Not all parameters can be estimated for every time step; some estimates cannot be obtained from sampling occasion one until sampling occasion two takes place, for example. Multiple formulations of the model were created with parameters either held constant through time or allowed to vary between time steps. A small–sample size corrected Akaike information criterion (AIC_c) was used for model selection, in which the lowest AIC_c value indicates the most parsimonious model based on several model parameters. Because this approach evaluates only model performance based on parsimony without respect to the likely realism of estimates, model estimates were secondarily evaluated on how well they appeared to approximate actual numbers of fish observed in the field. All population analyses were conducted using the RMARK software package (Laake 2013) within the R computing environment (R Core Team 2023).

2.2.3 Fish Health

In 2023, the health of largemouth bass in RQ was assessed by visually evaluating the external of the fish for abnormalities (e.g., apparent deformities, injuries, fin irregularities, and skin and gill parasites), meristic measurements, and condition factor. Because most fish in this study were marked and returned to the water for an ongoing mark-recapture study, most of the external visual abnormality assessments were conducted in the field. Fish with suspected deformities and fish being used for bioaccumulation studies were brought back to the laboratory for further examination (Figure 2).

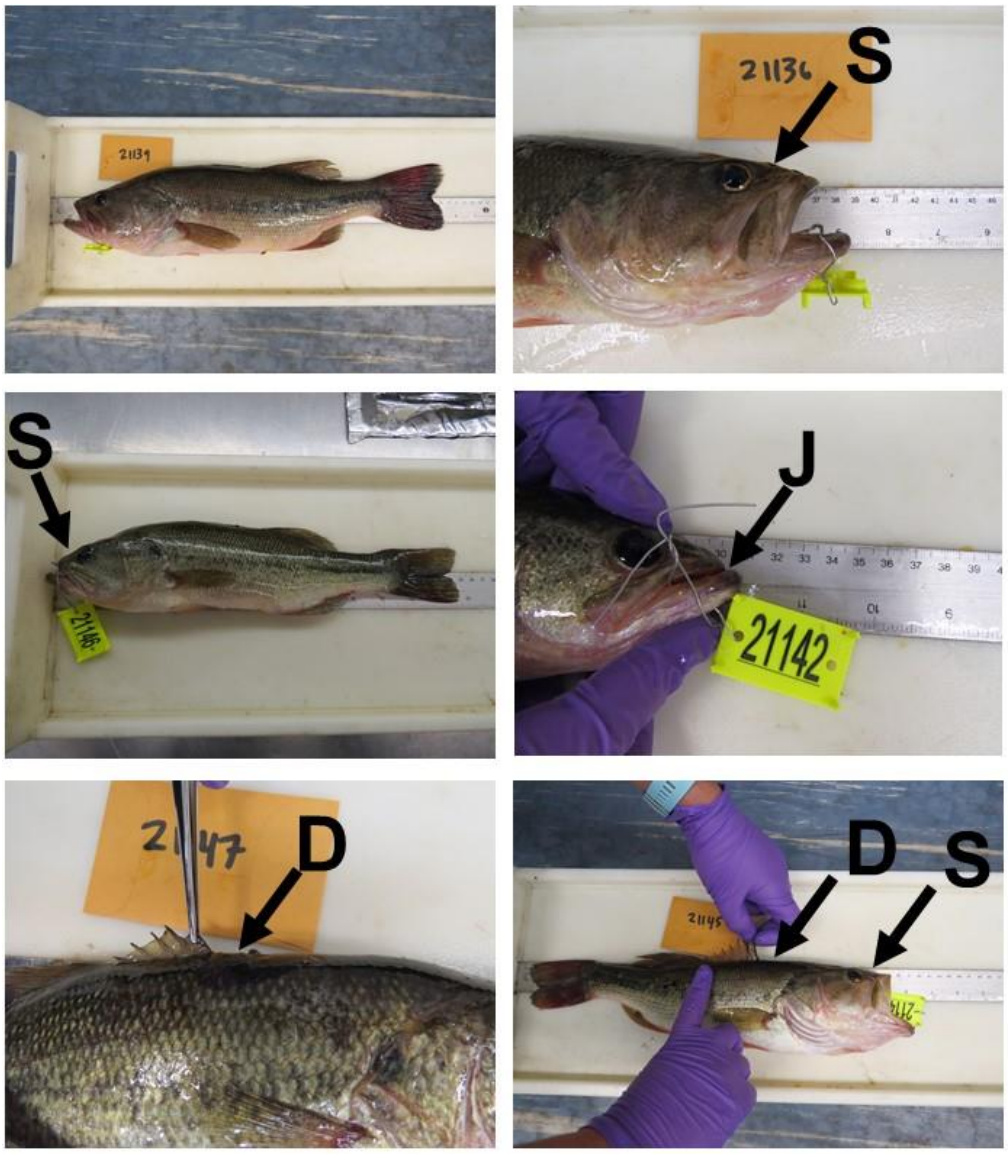

Figure 2. Typical deformities of Rogers Quarry largemouth bass collected in April 2017, including (S) a shortened rostral length, (J) protruding lower jaw, and (D) missing anterior portion of the dorsal fin. A putatively normal fish is shown in the top left image.

Fish meristic measurements—measurements between physical landmarks on a fish, such as the front of the eye to the opercle margin, that can be used to quantify physical characteristics of fish—were conducted on all largemouth bass brought back to the laboratory. Meristic measurements (Figure 3) were conducted as described by Perea et al. (2016) from photographs of fish taken with standardized position and lighting conditions.

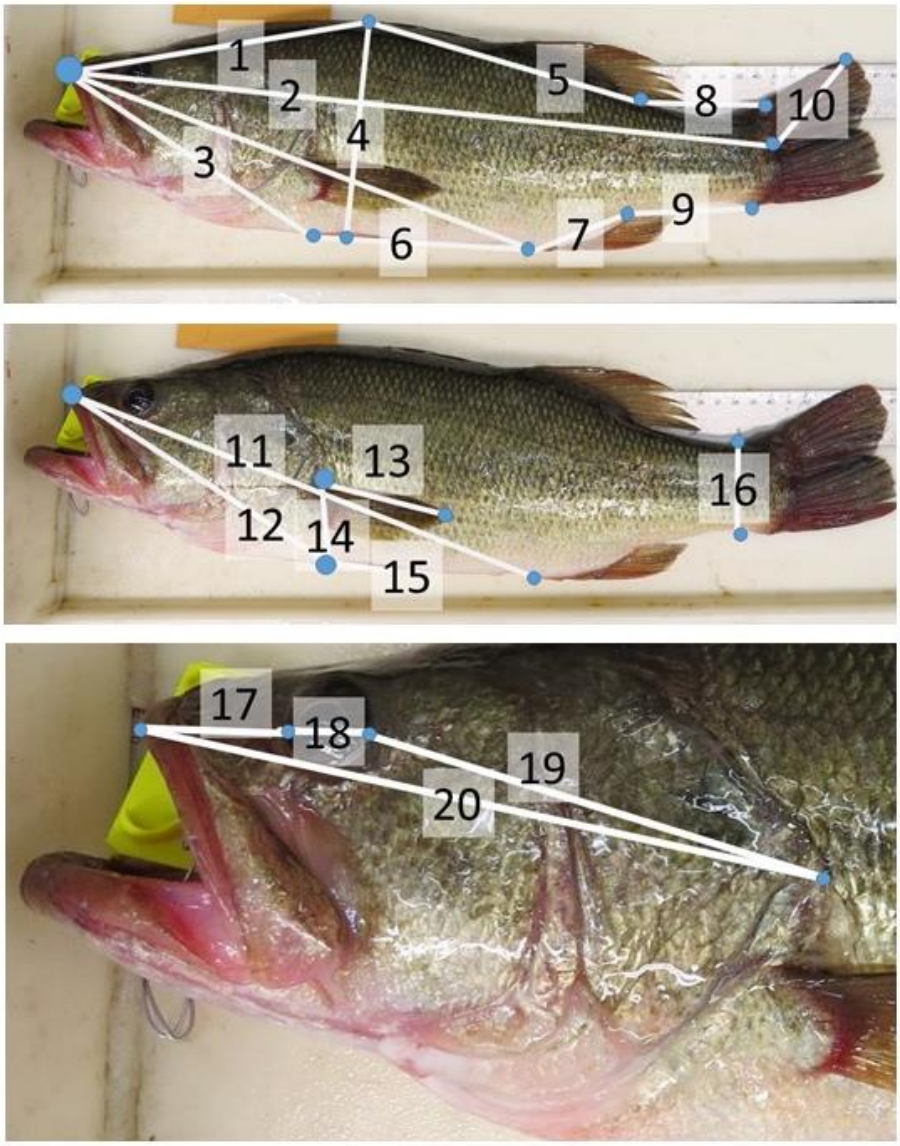

Figure 3. Meristic measurements made on largemouth bass collected from Rogers Quarry in April 2017. (1) Pre-dorsal distance, (2) body length, (3) prepectoral distance, (4) body depth, (5) dorsal fin length, (6) ventral–anal distance, (7) anal fin length, (8) caudal peduncle length, (9) anal peduncle length, (10) caudal fin length, (11) preanal distance, (12) preventral distance, (13) pectoral fin length, (14) pectoral–ventral length, (15) ventral fin length, (16) least body depth, (17) preorbital distance, (18) eye diameter, (19) postorbital distance, and (20) head length.

Methods to determine fish condition included Fulton's condition factor, *K*, calculated as

$$K = \frac{W}{L^3} \times 100, \quad (1)$$

where *W* is the total wet weight of the fish, and *L* is the total length of the fish. Fulton's condition factor was measured on all fish, including those not taken back to the laboratory.

3. RESULTS

3.1 WATER QUALITY SAMPLES

3.1.1 Total and Dissolved Hg

Concentrations of Hg_T and Hg_D were high throughout MB and RQ compared with previous years; all values were greater than 9 ng/L (Figure 4). About 80% of the total Hg was present as dissolved Hg. Concentrations of both parameters were, on average, more than 10 times higher than those measured in previous years. Dissolved Hg concentrations along McCoy Branch in 2023 were comparable to those measured in East Fork Poplar Creek (EFPC) at the Horizon Center (EFPC kilometer 5.4). Contemporaneous equipment blanks were at or below the method reporting limit, indicating that labware, sample storage containers, and preservatives did not contaminate samples. The concentration increase cannot be explained by higher suspended solids associated with antecedent rainfall (Table 2) because the TSS concentrations were in close agreement with those of previous years (Figure 4). However, given that most of the Hg was dissolved, these results may suggest precipitation-driven Hg mobilization from other, as yet unidentified, areas to MB via subsurface flowpaths.

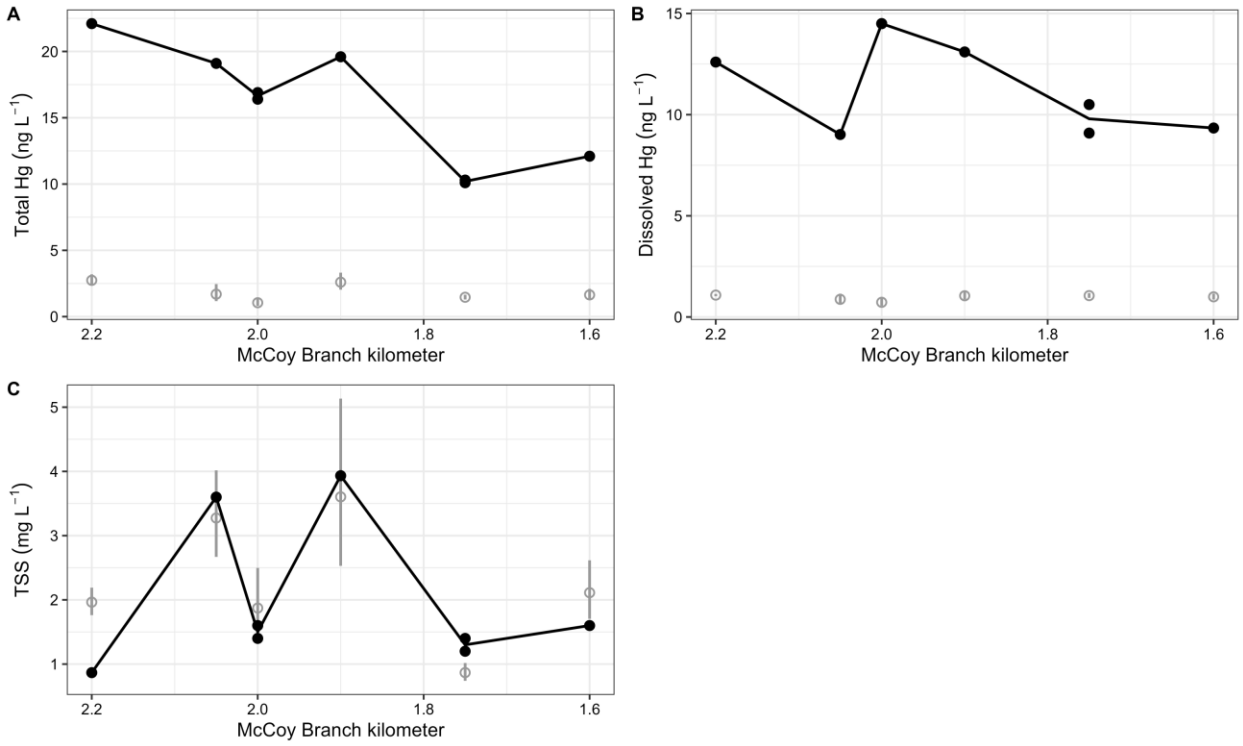

Figure 4. (A) Total Hg, (B) dissolved Hg, and (C) total suspended solids concentrations along McCoy Branch. Direction of flow is from left to right on the figures. Rogers Quarry surface water samples were taken at McCoy Branch kilometer 1.75. Filled symbols represent results from 2023. Open symbols represent the geometric mean (± standard error) of results from previous years.

Within RQ, Hg_T and Hg_D concentrations were 3.5 to 10 times higher than in previous years, and the concentration trends with depth were similar to trends seen in previous campaigns (Figure 5). About 90% of the total Hg was present as dissolved Hg. Like MB, the concentration increase cannot be explained by

higher suspended solids associated with antecedent rainfall because the TSS concentrations were in close agreement with previous years.

Although the elevated Hg concentrations in MB may reflect acute effects of recent rainfalls, higher concentrations throughout the 30-m water column in RQ suggest that Hg concentrations in MB were higher than normal for an extended period of time before sampling.

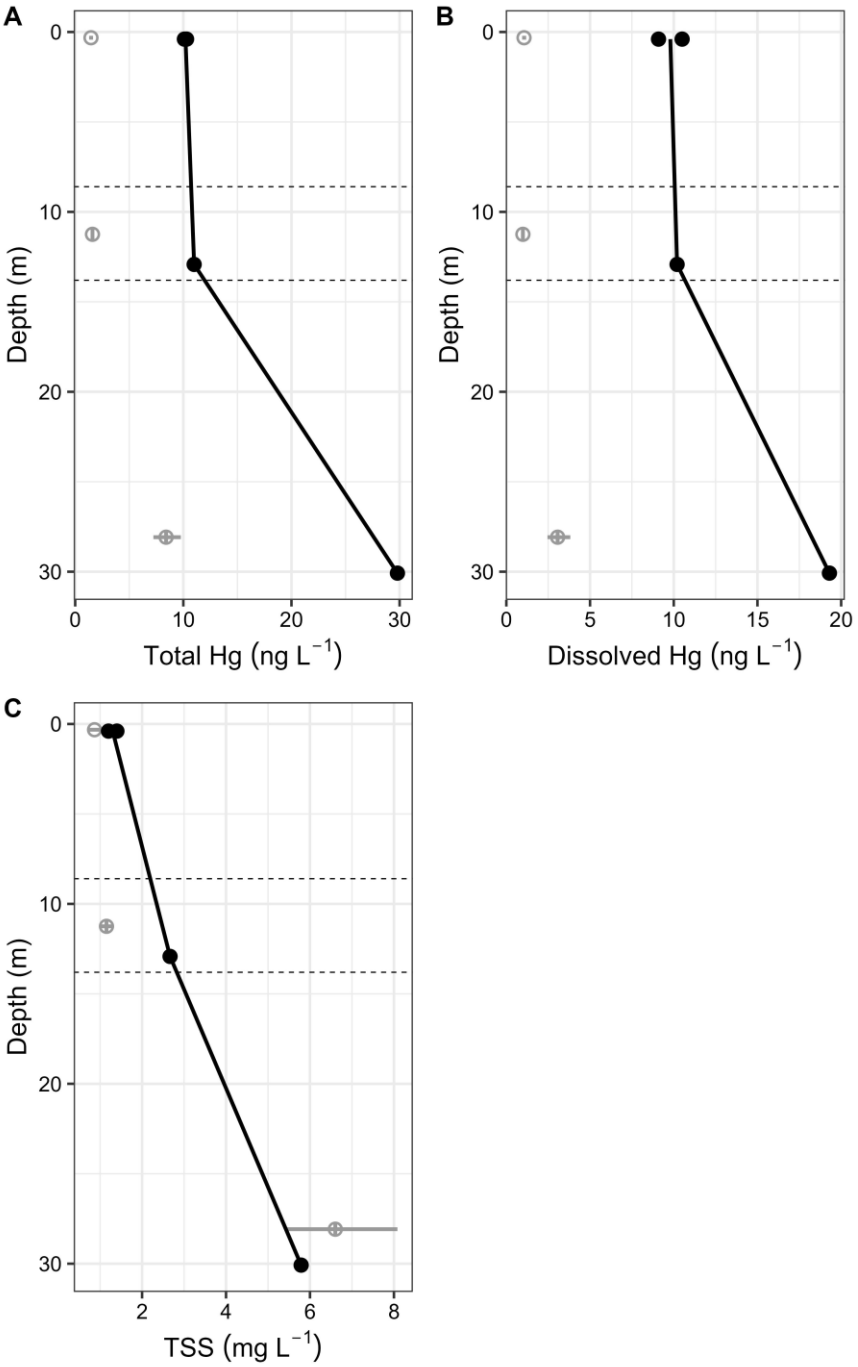

Figure 5. (A) Total Hg, (B) dissolved Hg, and (C) total suspended solids concentrations in Rogers Quarry as a function of depth. The horizontal dashed lines on each graph indicate the range of thermocline depths for all sampling campaigns. Filled symbols represent results from 2023. Open symbols represent the geometric mean (± standard error) of results from previous years.

3.1.2 Total and Dissolved MeHg

Most of the $MeHg_T$ or $MeHg_D$ results for samples collected along MB were below or very close to the reporting limit (0.05 ng·L^{-1}; Figure 6). The notable exception was the sample collected from the FCAP (MCK 2.2) in which the $MeHg_T$ and $MeHg_D$ concentrations were well above reporting limits and, importantly, were comparable to those measured in EFPC at the Horizon Center (EFPC kilometer 5.4).

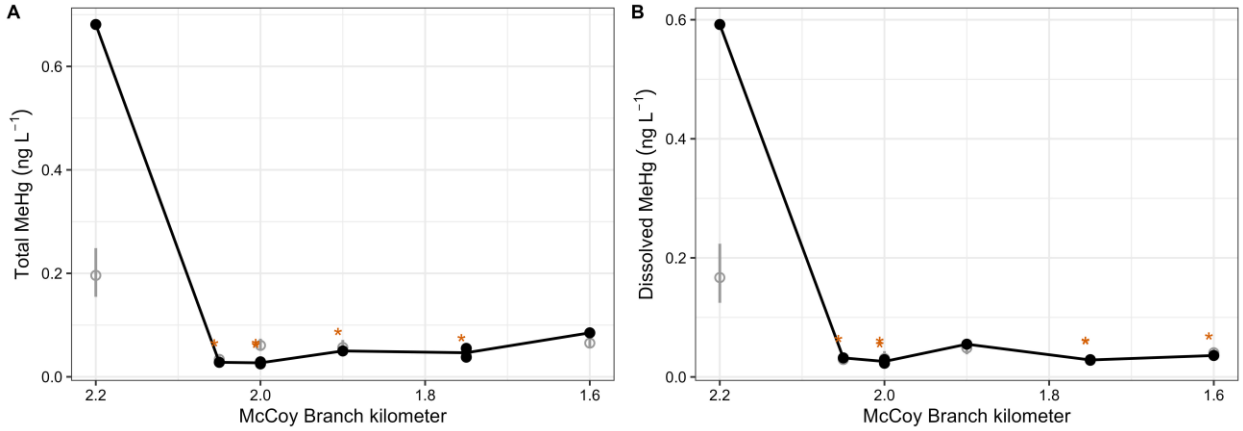

Figure 6. (A) Total MeHg and (B) dissolved MeHg concentrations along McCoy Branch. Direction of flow is from left to right on the figures. Filled symbols represent results from 2023. Open symbols represent the geometric mean (± standard error) of results from previous years. Asterisks adjacent to symbols indicate the result from 2023 was below reporting limits.

Within RQ, the pattern in $MeHg_T$ and $MeHg_D$ concentrations closely mirrored those measured in previous years—low concentrations in surface water and thermocline samples and higher concentrations in samples from the quarry bottom (Figure 7). The $MeHg_T$ concentration (3.63 ng·L^{-1}) and $MeHg_D$ concentration (4.53 ng·L^{-1}) in samples from the quarry bottom were substantially higher than the concentrations in samples collected from shallower depths. The concentrations in these deep samples were also substantially higher than those in EFPC. Section 3.1.1 hypothesizes potential explanations of higher $MeHg_T$ concentration in the deep sample. Elevated MeHg concentration in these deep samples is consistent with anoxic conditions typically measured in samples from that depth. RQ is thermally stratified (Section 3.1.3), which limits the amount of vertical mixing between the deeper, anoxic, high-MeHg waters and the shallower, oxic, low-MeHg waters where fish reside. Long-term temperature monitoring suggests that the quarry waters turn over at least once a year (Section 3.1.3), when the deeper water mixes with the shallower water.

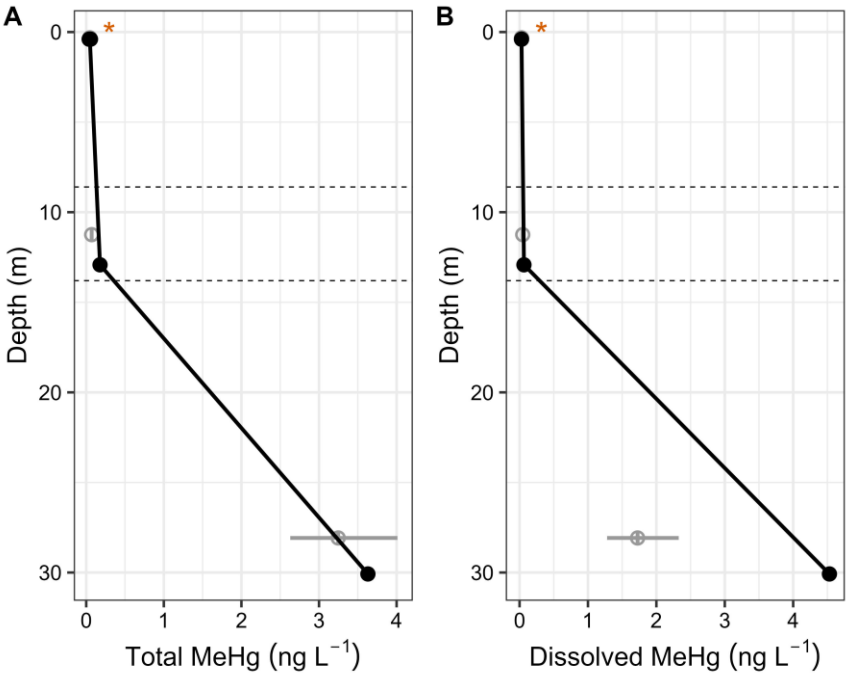

Figure 7. (A) Total MeHg and (B) dissolved MeHg$_D$ concentrations in Rogers Quarry as a function of depth. The horizontal dashed lines on each graph indicate the range of thermocline depths for all sampling campaigns. Filled symbols represent results from 2023. Open symbols represent the geometric mean (± standard error) of results from previous years. Asterisks adjacent to symbols indicate the result from 2023 was below reporting limits.

3.1.3 Field-Measured Parameters

Field-measured parameters (temperature, pH, specific conductance, and DO) for surface water along MB varied within a range typical for local streams and closely matched the several-year average in both magnitude and along-creek pattern (Figure 8). DO concentrations were notably lower in water on the FCAP and the seepage outlet at the base of the 19 m high earthen dam at MCK 2.05. DO levels increase rapidly downstream of that site and remain high. High water temperature at MCK 1.6 is consistent with the lack of canopy or riparian shading and the low flow and shallow water depth.

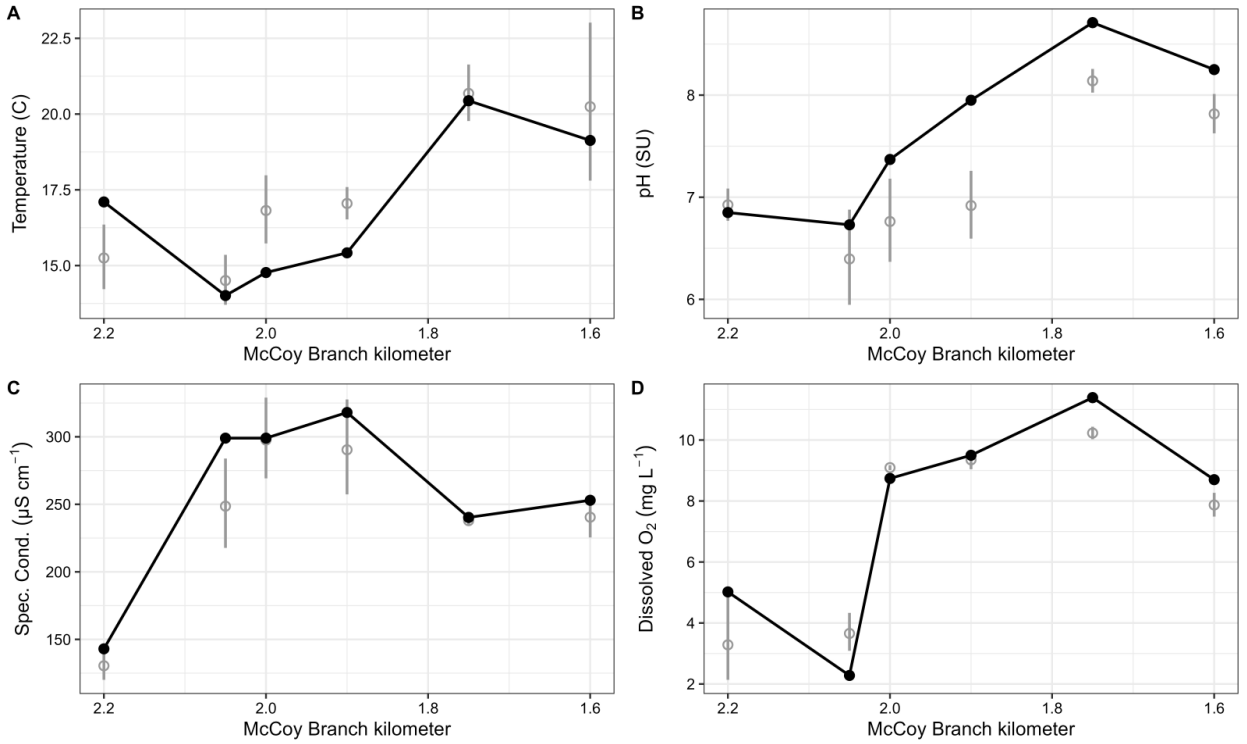

Figure 8. Field parameters along McCoy Branch. Filled symbols represent results from 2023. Open symbols represent the geometric mean (± standard error) of results from previous years. (Note: Spec. Cond. = specific conductance.)

Field parameters as a function of depth in RQ followed the general trends observed in previous years (Figure 9). Temperature data showed a thermally stratified water body with warmer surface water overlying colder, deeper water and a thermocline at approximately 13 m. Steep gradients of increasing specific conductance, decreasing pH, and decreasing DO coincide with the thermocline. Turbidity was relatively constant with depth until the deepest parts of the quarry were reached. The high turbidity values recorded for the deepest samples are likely the result of disturbing the bottom sediments with the sonde. High turbidity in surface waters of RQ in April 2017 was caused by heavy rains and overland runoff in the days before sampling.

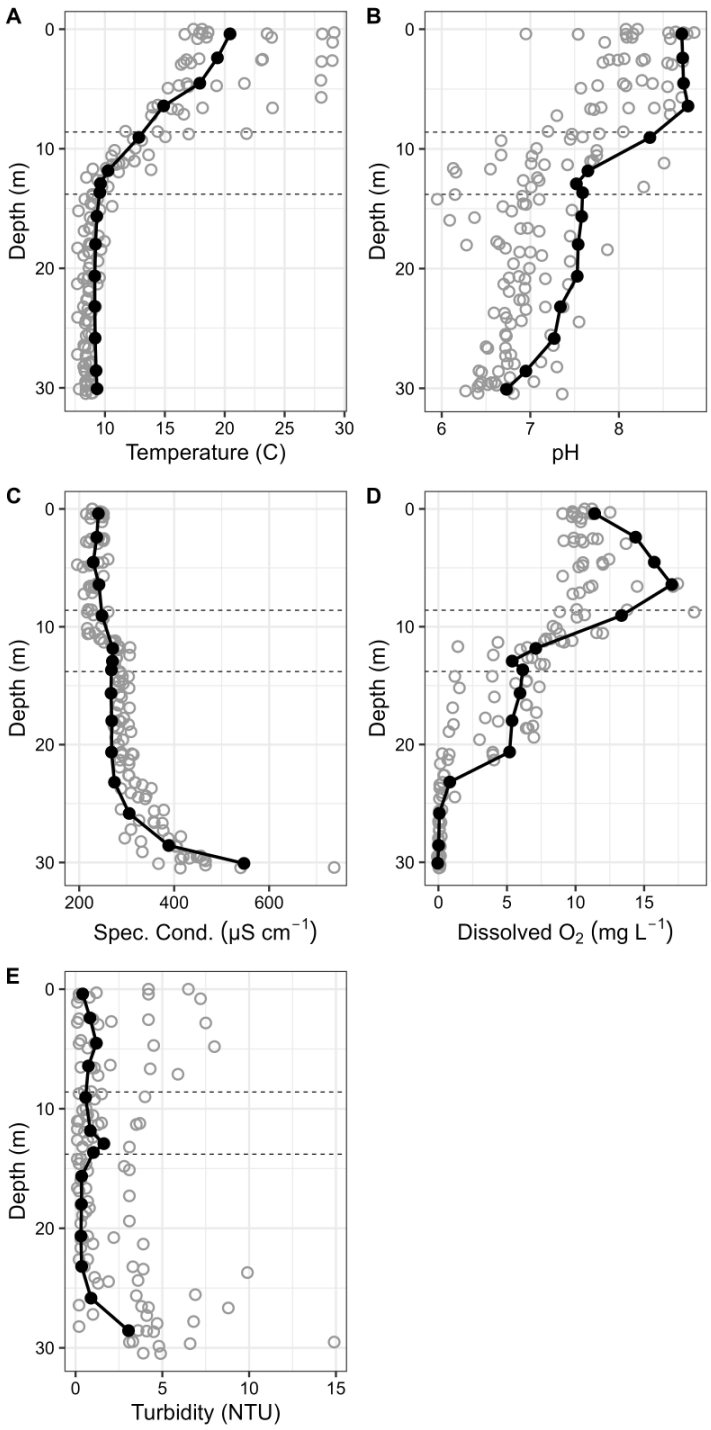

Figure 9. Field-measured parameters as a function of depth in Rogers Quarry for each sampling campaign. Filled symbols connected by a solid line represent the 2023 measurements. Open symbols are measurements from previous years. High turbidity values at the deepest depths are likely artifacts of disturbing bottom sediments with the sonde. One turbidity value of 73 NTU at 30 m deep is not shown. The horizontal dashed lines on each graph indicate the range of thermocline depths for all sampling campaigns. (Notes: Spec. Cond. = specific conductance, NTU = nephelometric turbidity units.)

Because of the marked differences in water quality between the surface and deeper waters in RQ, a vertical temperature sensor array was deployed to measure and record water temperature at 30 min intervals from August 2017 to June 2018. A strong temperature gradient with depth was recorded in the summer and early fall (Figure 10). That gradient weakened into the winter, with uniform temperatures with depth achieved in January and February, and the gradient reestablished through the spring. Uniform water temperature with depth is significant because it suggests that conditions would allow the anoxic deeper waters (higher in Hg_T, $MeHg_T$, and total As) to mix with the shallower waters, thus creating a potential exposure pathway for receptors in the upper levels of RQ and downstream in MB. Nevertheless, potential density effects caused by higher dissolved solids concentration as suggested by the specific conductance data (Figure 9C) may decrease or prevent such mixing. New sampling campaigns would be needed to confirm seasonal vertical mixing in RQ.

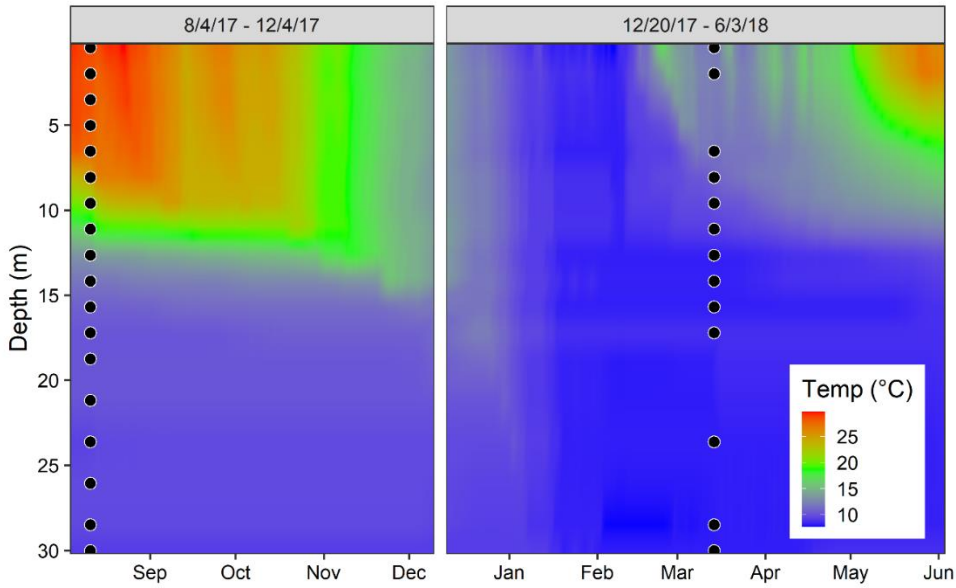

Figure 10. Rogers Quarry water temperature measured with depth from August 2017 to June 2018. The temperature gradient with depth declined through fall 2017, until uniform temperatures were achieved in January and February 2018. The temperature gradient formed again through spring 2018. Symbols on each panel indicate the depths at which temperature data were collected. A few of the sensors failed in mid-March 2018.

3.1.4 Anions, Ferrous Iron, Sulfide, and Trace Metals

Surface water longitudinal profile. Major anion concentrations in the surface water samples along MB and RQ were typical for local streams and were consistent with the overall average values from previous years (Figure 11). Some of the high variability associated with historical results was caused by a dilution effect imparted by sampling after heavy rains. Total Fe and ferrous iron were below detection limits in all surface water samples. Sulfide was detected in water samples collected from the artificial wetland (MBK 2.05 = 5.4 µg L^{-1}) and the next downstream sampling location (MBK 2 = 5.6 µg L^{-1}).

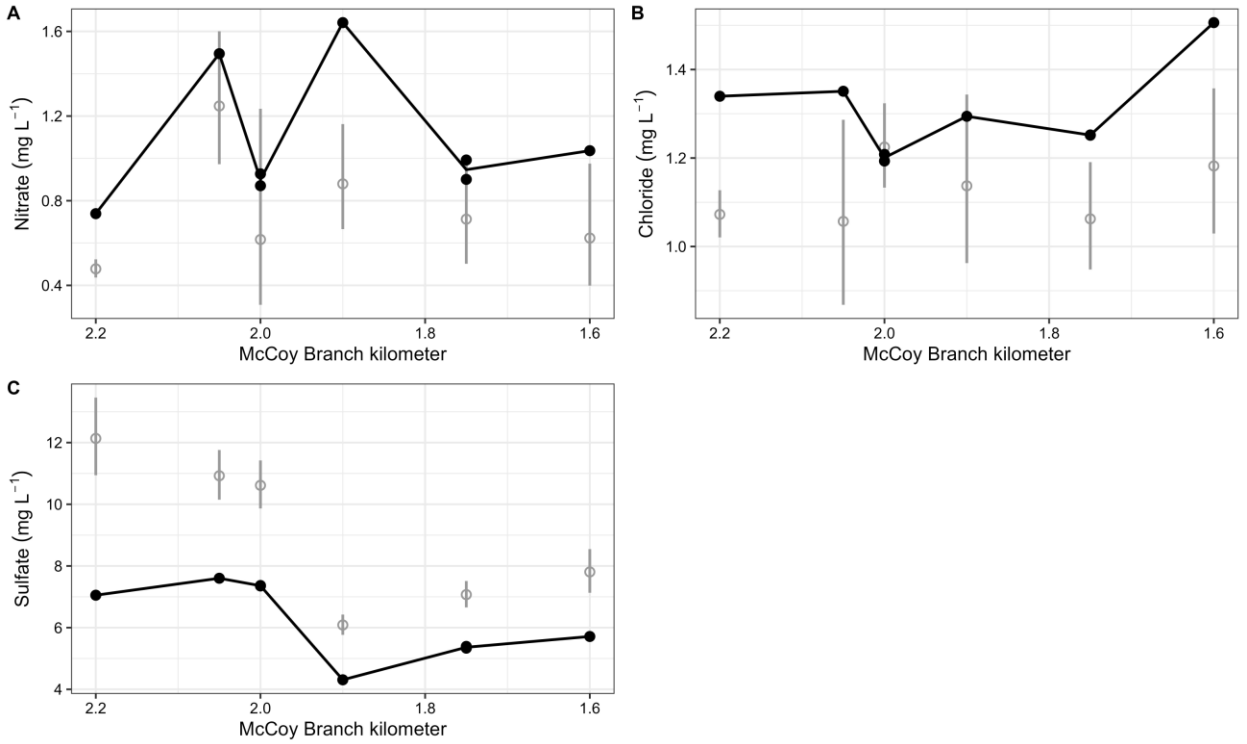

Figure 11. Concentrations of (A) nitrate, (B) chloride, and (C) sulfate along McCoy Branch.
Filled symbols represent results from 2023. Open symbols represent the geometric mean (± standard error) of results from previous years.

RQ depth profile. Chloride concentration was low and relatively uniform with depth in RQ within each sampling event, although concentrations varied among sampling events (Figure 12). Nitrate concentrations also were low and, interestingly, displayed a maximum concentration at the thermocline. Sulfate concentrations were similar in the surface and thermocline samples and were lowest in the deepest sample. Sulfide was present above reporting limits (5.1 µg L^{-1}) in the sample collected from the deepest depth with a value of 9 µg L^{-1}.

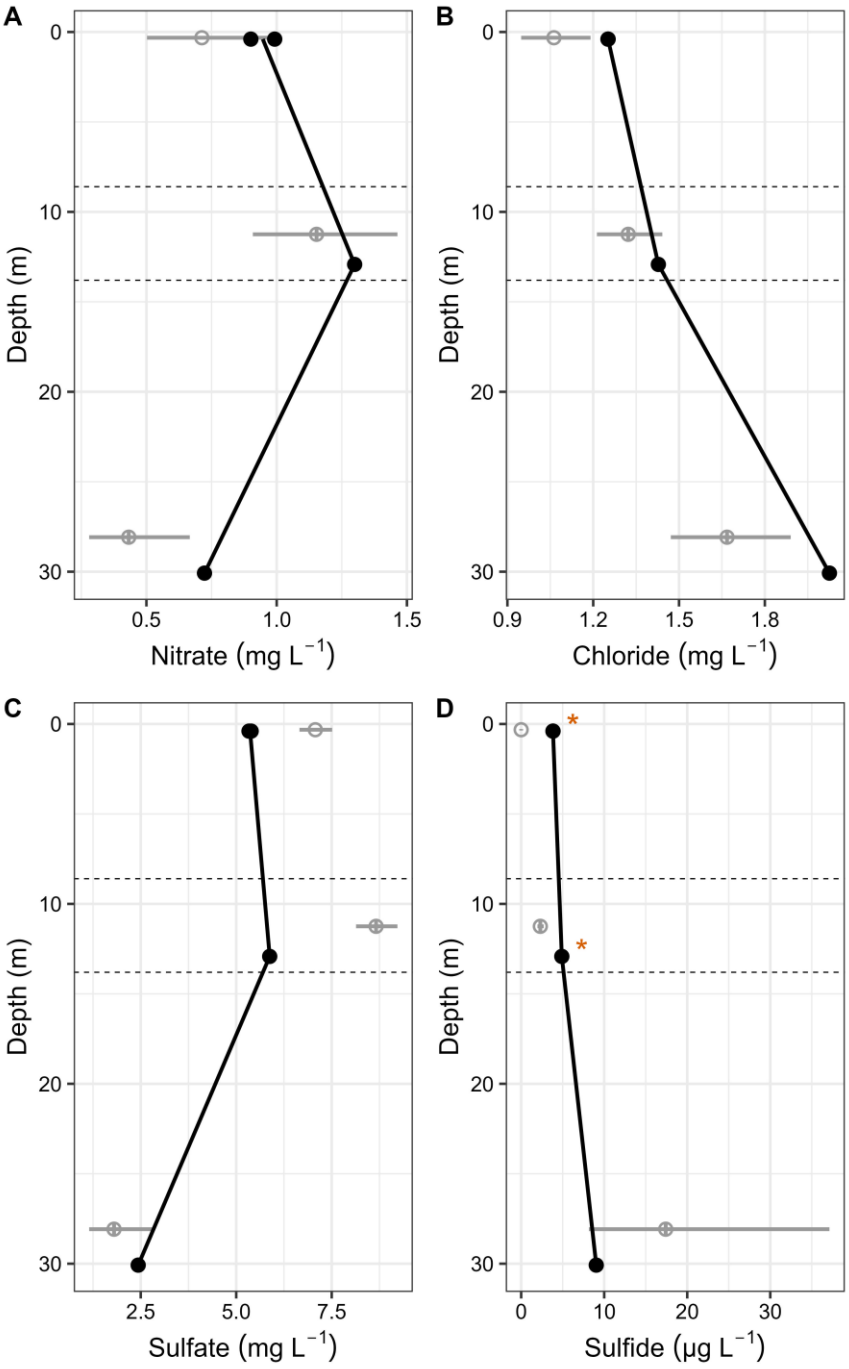

Figure 12. Concentrations of (A) nitrate, (B) chloride, (C) sulfate, and (D) sulfide with depth in Rogers Quarry. The horizontal dashed lines on each graph indicate the range of thermocline depths for all sampling campaigns. Filled symbols represent results from 2023, and open symbols represent the geometric mean (± standard error) from previous years. Asterisks adjacent to symbols indicate the result from 2023 was below reporting limits.

Sampling for CH_4 should be considered for future sampling campaigns because the presence of CH_4 would indicate whether the system has progressed through sulfate reduction (as suggested by the absence of sulfate at depth in previous years) to methanogenesis. This progression would be significant because a dominant Hg-methylating microbial taxon (*Archaea*) includes the methanogens.

3.1.5 Se and As

Surface water longitudinal profile. Total and dissolved As concentrations exceeded the EPA drinking water standard (10 µg·L^{-1}) in samples collected from MCK 2.05 and decreased rapidly with distance downstream (Figure 13). More than 85% of total As was dissolved (i.e., passed a 0.2 µm pore size filter) throughout MB for the samples collected in 2023 with the exception of MCK 2.05, where dissolved As constituted 25% of the total As. The concentration patterns along MB for samples collected in 2023 were similar to those from previous years.

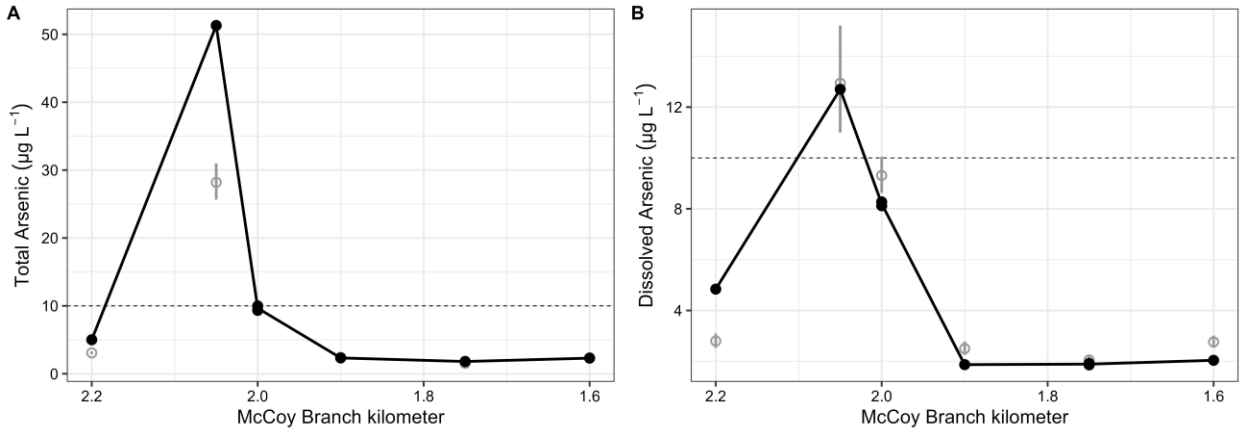

Figure 13. (A) Total and (B) dissolved As concentrations along McCoy Branch and Rogers Quarry. The US Environmental Protection Agency drinking water standard for As (10 µg·L^{-1}) is indicated by the dashed horizontal line. Direction of flow is from left to right on the figures. Filled symbols represent results from 2023. Open symbols represent the geometric mean (± standard error) of results from previous years.

Over time, total As concentrations in water have varied depending on location along MB (Figure 14). The arsenic concentration-versus-time data have been filtered to include only those results from Brooks Applied Labs. At the three farthest downstream locations (MCK 1.6, 1.75, and 1.9), total As concentrations have been consistently low with little change over time. Samples collected at MCK 2.0 decreased over the first two years and currently hover around the EPA drinking water standard. Samples collected at MCK 2.05, the wetland area below the FCAP, initially declined but then increased substantially. Concentrations at the FCAP (MCK 2.2) may be slowly increasing—data gaps due to dry conditions during several sampling years make the possible trend uncertain. Trends in dissolved As concentrations over time are broadly similar to those described for total As with the exception of concentrations at the wetland (MCK 2.05), which declined sharply between 2019 and 2020 and have remained steady since then.

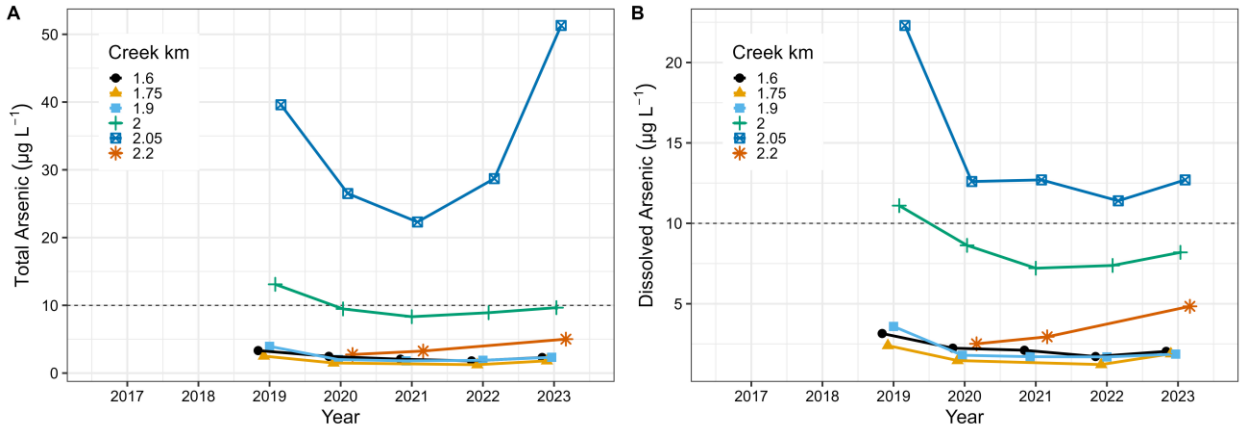

Figure 14. (A) Total and (B) dissolved As concentrations along McCoy Branch over time. The US Environmental Protection Agency drinking water standard for As (10 µg·L^{-1}) is indicated by the dashed horizontal line. Symbols represent the geometric mean (± standard error). Results have been "jittered" on the x-axis to improve readability.

For samples collected along MB, total and dissolved Se concentrations were below the EPA aquatic life ambient water quality criterion for lotic ecosystems (3.1 µg·L^{-1}). Concentrations decreased from MCK 2.05 to MCK 1.9 and remained relatively constant farther downstream. Virtually all Se (>98%) was dissolved (Figure 15).

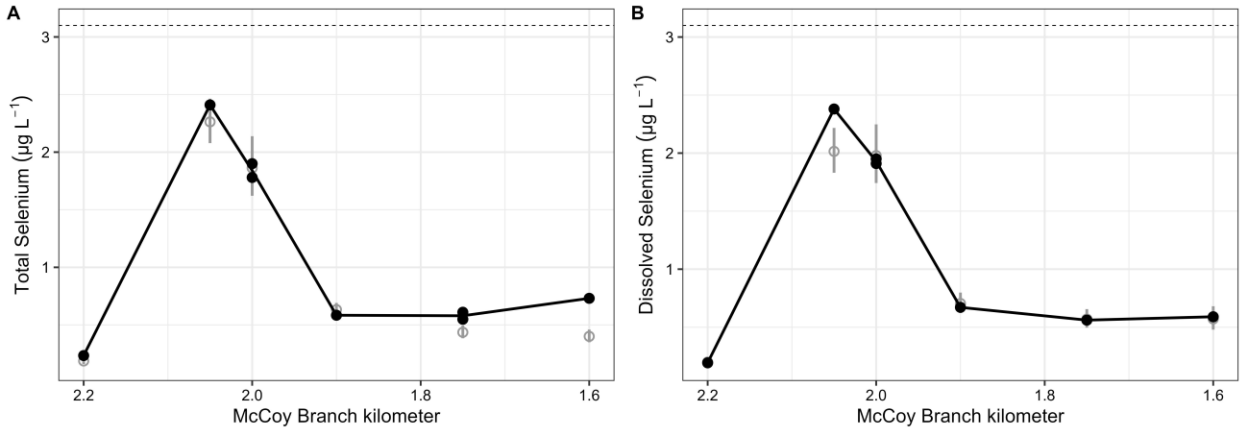

Figure 15. (A) Total and (B) dissolved Se concentrations along McCoy Branch. The US Environmental Protection Agency aquatic life ambient water quality criterion for Se in freshwater lotic ecosystems (3.1 µg·L^{-1}) is indicated by the dashed horizontal line. Direction of flow is from left to right on the figures. Filled symbols represent results from 2023. Open symbols represent the geometric mean (± standard error) of results from previous years. Asterisks adjacent to symbols indicate the result from 2023 was below reporting limits.

Total and dissolved Se concentrations in water samples from MB show no strong temporal patterns (Figure 16). The selenium concentration-versus-time data have been filtered to include only those results from Brooks Applied Labs. Concentrations are higher and more variable in samples collected from the wetland (MCK 2.05) and at the first location downstream from the wetland (MCK 1.9).

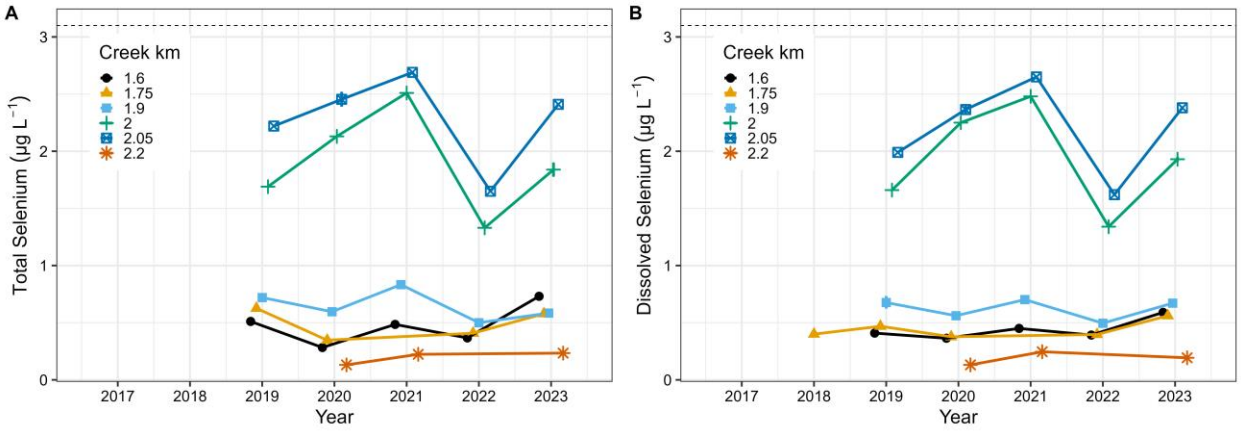

Figure 16. (A) Total and (B) dissolved Se concentrations along McCoy Branch over time. The US Environmental Protection Agency aquatic life ambient water quality criterion for Se in freshwater lotic ecosystems (3.1 µg·L^{-1}) is indicated by the dashed horizontal line. Symbols represent the geometric mean (± standard error) of results and have been "jittered" on the x-axis to improve readability.

RQ depth profile. Total and dissolved As concentrations increased with depth in RQ, and all results were below the EPA drinking water standard (10 µg·L^{-1}; Figure 17). Of the total As, 100% was dissolved.

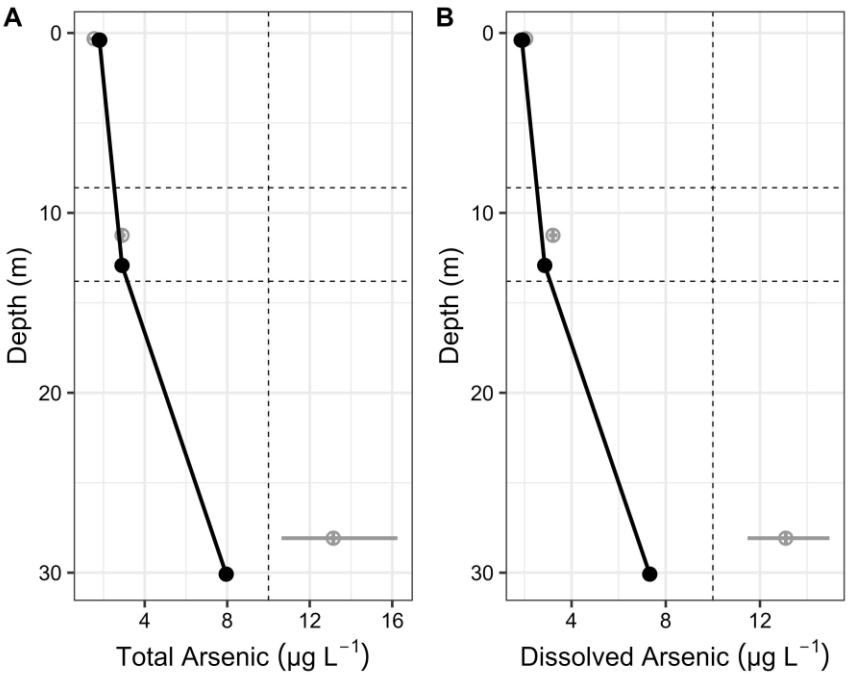

Figure 17. (A) Total and (B) dissolved As concentrations plotted with depth in Rogers Quarry. The US Environmental Protection Agency drinking water standard for As (10 µg·L^{-1}) is indicated by the dashed vertical line. The horizontal dashed lines on each graph indicate the range of thermocline depths for all sampling campaigns. Filled symbols represent results from 2023. Open symbols represent the geometric mean (± standard error) of results from previous years.

Over time, As concentrations in surface water and thermocline samples from RQ have been low, well below the EPA drinking water standard, and relatively stable (Figure 18). Arsenic concentrations in water samples collected near the bottom of RQ have been consistently substantially higher than concentrations in samples from the surface or thermocline. In 2019 and 2020, As concentrations in these deep samples were above the EPA drinking water standard; in recent years, the concentrations have been below that limit and now may be slowly decreasing.

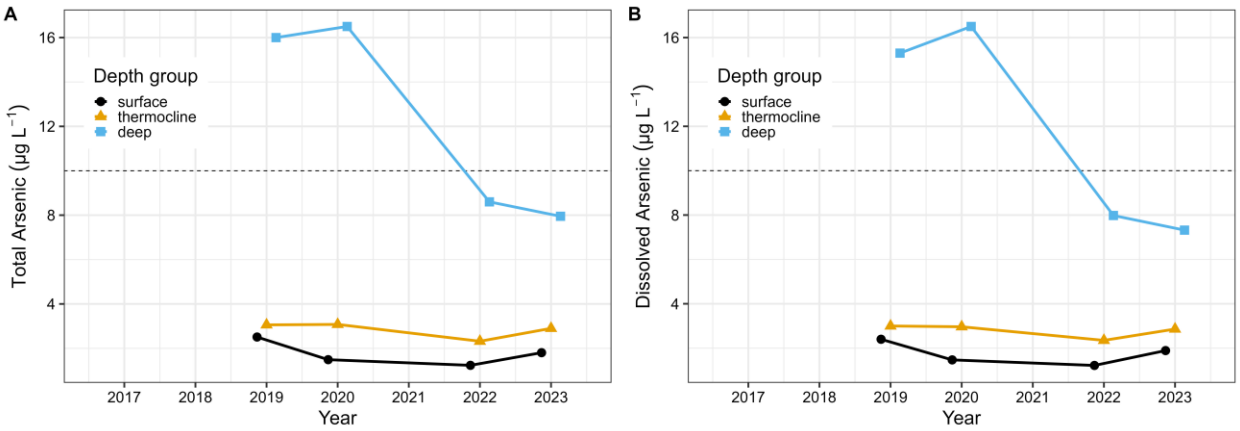

Figure 18. (A) Total and (B) dissolved As concentrations in Rogers Quarry over time. The US Environmental Protection Agency drinking water standard for As (10 µg·L^{-1}) is indicated by the dashed horizontal line. Symbols represent the geometric mean (± standard error). Results have been "jittered" on the x-axis to improve readability.

Total and dissolved Se concentrations decreased with depth in RQ, and all results were below the EPA aquatic life ambient water quality criterion for lentic ecosystems (1.5 µg·L^{-1}; Figure 19). More than 90% of the total Se was dissolved. The overall results and concentration versus depth patterns for As and Se were consistent with results from previous years.

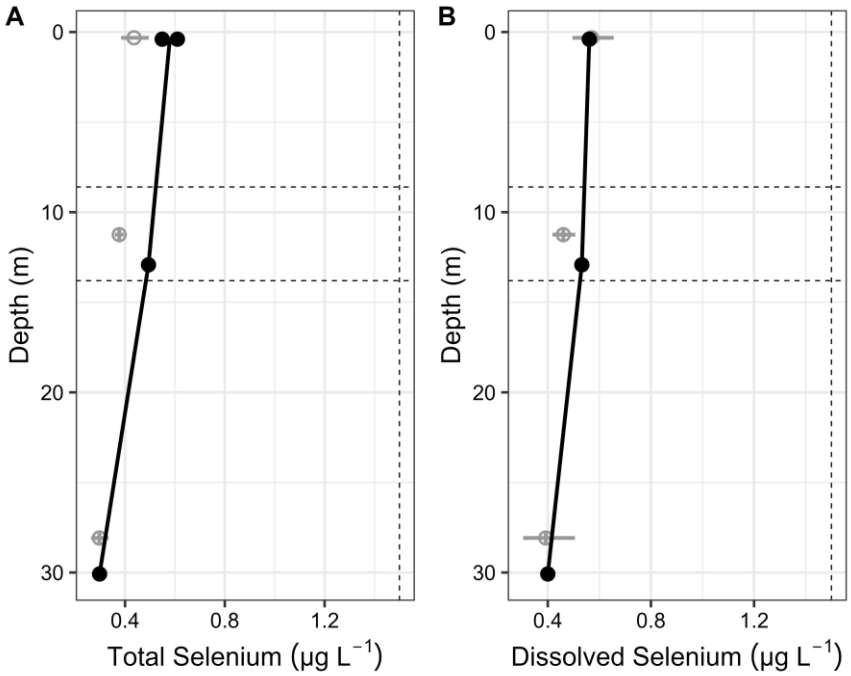

Figure 19. (A) Total Se and (B) dissolved Se concentrations plotted with depth in Rogers Quarry. The US Environmental Protection Agency aquatic life ambient water quality criterion for Se in freshwater lentic ecosystems (1.5 µg·L^{-1}) is indicated by the dashed vertical line. The horizontal dashed lines on each graph indicate the range of thermocline depths for all sampling campaigns. Filled symbols represent results from 2023. Open symbols represent the geometric mean (± standard error) of results from previous years.

Selenium concentrations in RQ have not shown any strong temporal trend and have remained well below the relevant aquatic life ambient water quality criterion (Figure 20). Selenium concentrations in water samples collected from near the bottom of RQ are consistently lower than concentrations in samples collected from the surface or thermocline.

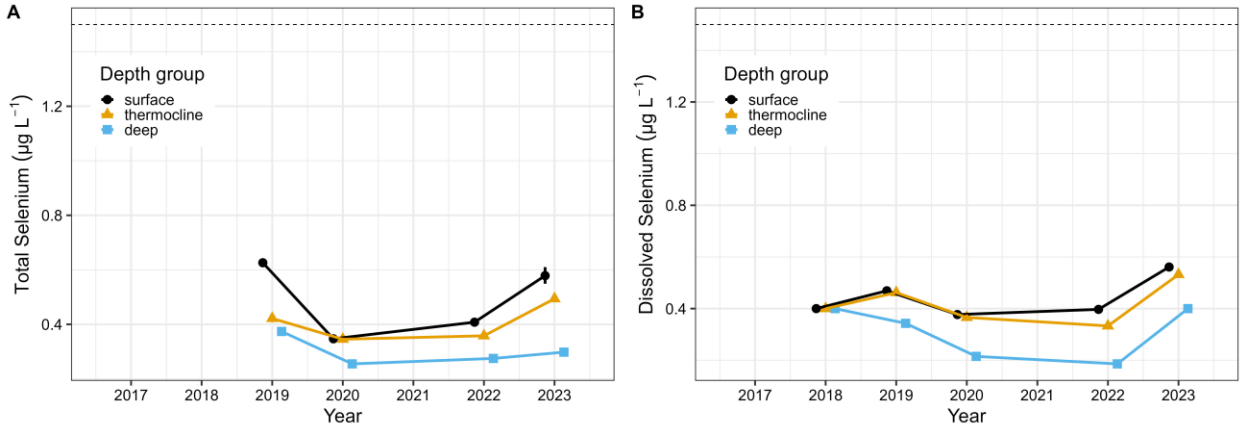

Figure 20. (A) Total and (B) dissolved Se concentrations in Rogers Quarry over time. The US Environmental Protection Agency aquatic life ambient water quality criterion for Se in freshwater lentic ecosystems (1.5 µg·L^{-1}) is indicated by the dashed horizontal line. Symbols represent the geometric mean (± standard error). Results have been "jittered" on the x-axis to improve readability.

3.2 SEDIMENTS, BANK SOILS, COAL ASH, AND BIOFILMS

Samples of creek sediment, bank soils, and benthic biofilms were collected along MB in 2023. Samples of legacy coal ash (determined based on visual appearance) exposed on creek banks were sampled in 2017 and 2020.

Mercury and Methylmercury. Total Hg concentrations in solid phases (bank soil, coal ash, biofilms, sediments) are low and generally decline along the length of MB (Figure 21). All values were well below the consensus-based sediment quality probable effect concentration (PEC) of 1.08 mg kgdw^{-1} (MacDonald et al. 2000). The Tennessee Department of Environment and Conservation references this PEC value when discussing streams on the Oak Ridge Reservation. The PEC is defined as the "concentration above which adverse effects are expected to occur more often than not" and the adverse effects are with respect to sediment-dwelling organisms in freshwater ecosystems. Total Hg concentration in biofilms ranged from 0.9× (MCK 2) to 2.1× (MCK 2.05) higher than concentrations measured in colocated creek sediments.

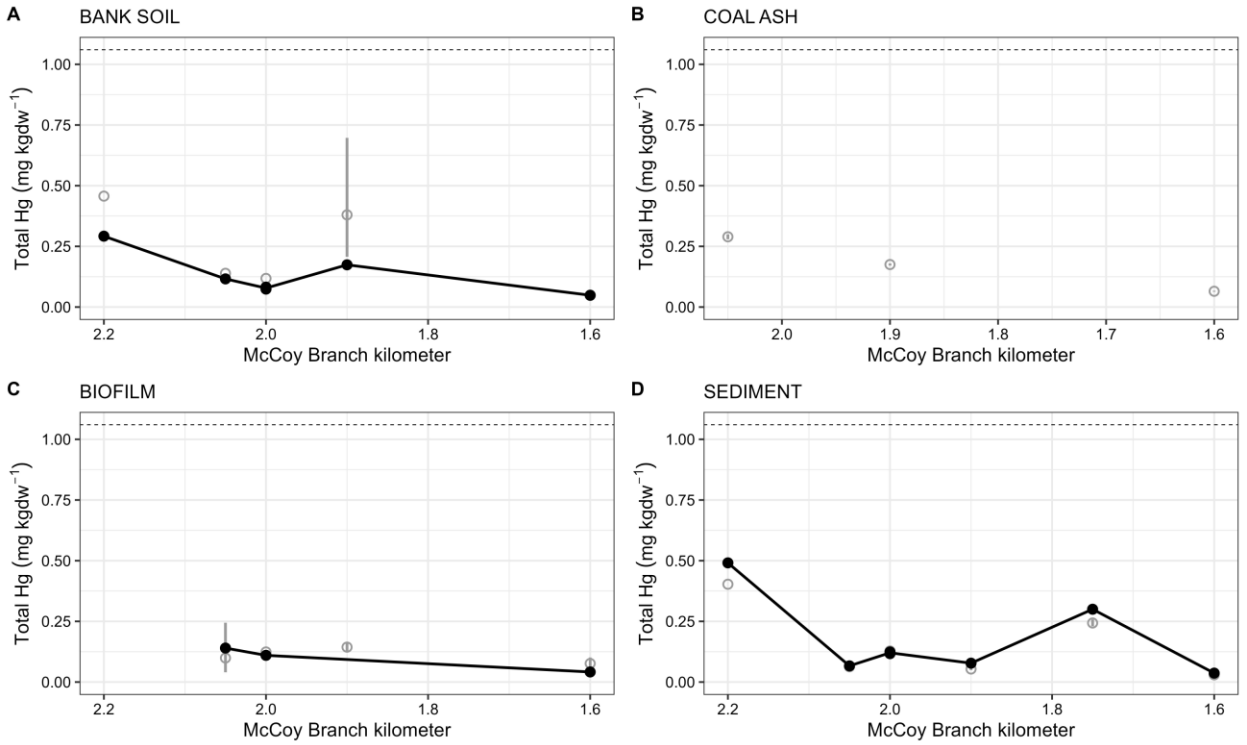

Figure 21. Total mercury concentrations along McCoy Branch in (A) bank soils, (B) coal ash in creek banks, (C) benthic biofilms, and (D) creek sediments. Probable effect concentration (1.06 mg kgdw^{-1}) is indicated by the dashed horizontal line. Filled symbols represent results from 2023. Open symbols represent the geometric mean (± standard error) of results from previous years. (Note: kgdw = kilogram dry weight.)

Total MeHg concentrations in solid phases varied among the materials. For example, concentrations in bank soils and coal ash were similar but differed in their spatial patterns where concentrations in bank soils generally declined along the length of MB and in coal ash concentrations that peaked in the upper third of the sampled reach (Figure 22). In contrast, MeHg concentrations in biofilms and sediments tended to increase along MB. Sediment MeHg concentrations in the lower half of the sample reach were comparable to those measured in EFPC near the Horizon Center. There are no existing or proposed MeHg sediment quality guidelines for freshwater ecosystems. Across all solids sampled in 2023, on average

MeHg constituted 2.9% of total Hg and ranged between 0.02% (sediment at MCK 2.05) and 32% (biofilms at MCK 1.6). Importantly, total MeHg concentration in biofilms ranged from 6.2× (MCK 2) to over 250× (MCK 2.05) higher than concentrations measured in colocated creek sediments reflective of (1) higher MeHg bioaccumulation and (2) biofilms as a source of MeHg production in streams.

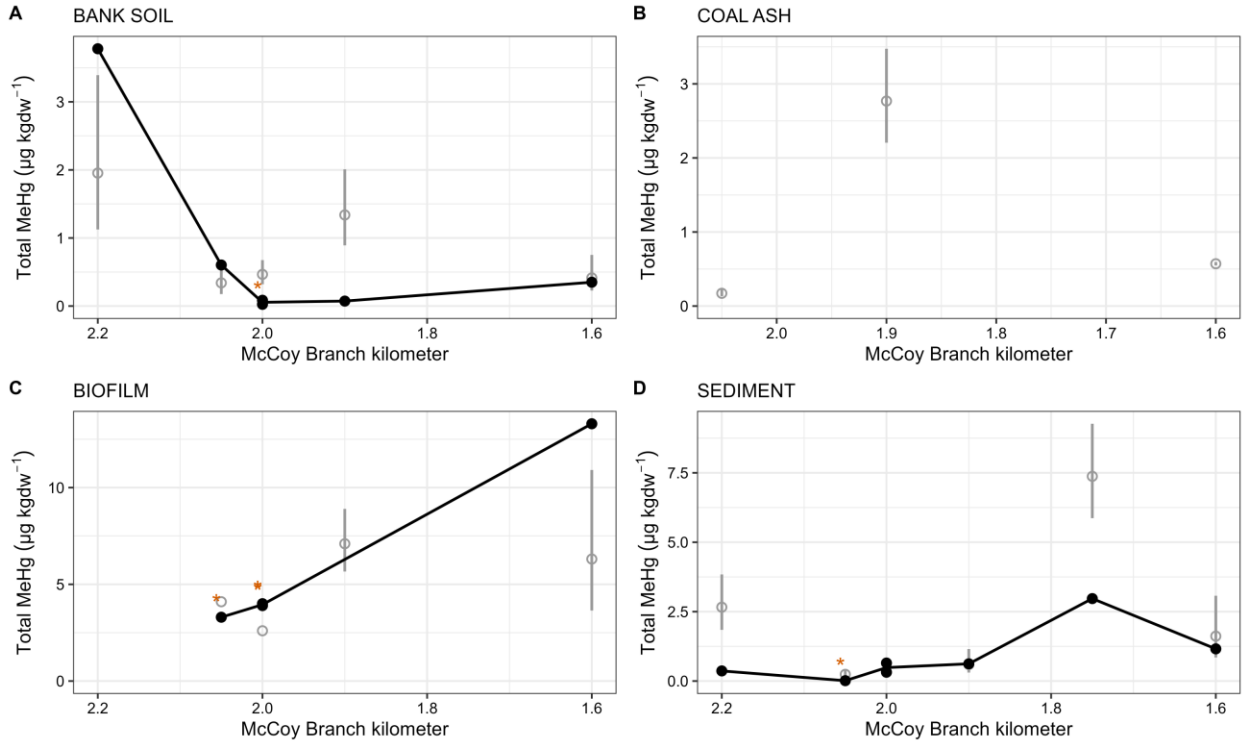

Figure 22. Total methylmercury concentrations along McCoy Branch in (A) bank soils, (B) coal ash in creek banks, (C) benthic biofilms, and (D) creek sediments. Filled symbols represent results from 2023. Open symbols represent the geometric mean (± standard error) of results from previous years. Asterisks adjacent to symbols indicate the result from 2023 was below reporting limits. (Note: kgdw = kilogram dry weight.)

Arsenic and selenium. Concentrations of As in creek sediments, bank soils, coal ash, and biofilms throughout much of MB and at the bottom of RQ exceeded the consensus-based PEC for freshwater ecosystems (33 mg kg^{-1}). The highest biofilm and sediment As concentrations were in samples from MCK 2.05, which is the location of the artificial wetland designed to remove As from the water (Figure 23). Notably, the biofilm concentration was orders of magnitude higher than the concentration in previous years, suggesting that the biofilm sample may have contained a large proportion of sediment. Nevertheless, the biofilm arsenic concentration at MCK 2.05 was 3.2× higher than that of the colocated sediments, possibly indicative of additional factors contributing to the high biofilm concentration.

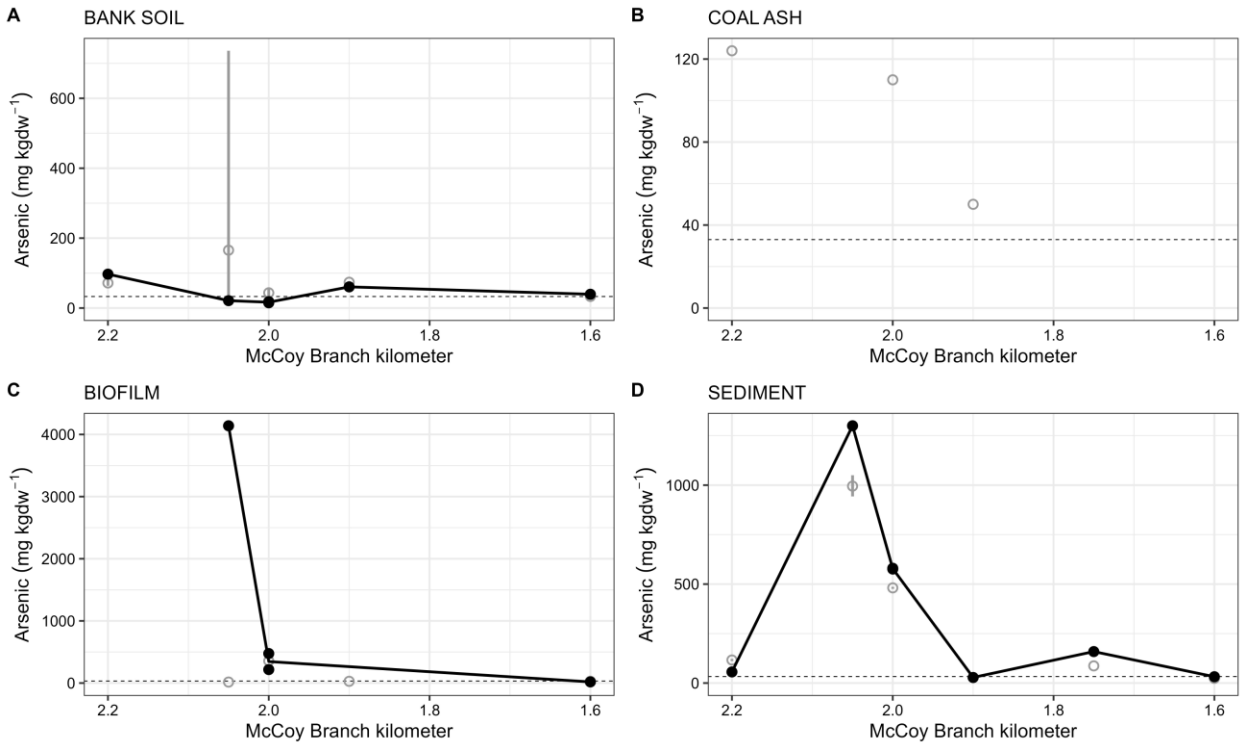

Figure 23. Arsenic concentrations along McCoy Branch in (A) bank soils, (B) coal ash in creek banks, (C) benthic biofilms, and (D) creek sediments. Filled symbols represent the results from 2023. Open symbols represent the geometric mean (± standard error) of results from previous years. The horizontal dashed line represents the probable effect concentration for As in freshwater sediments (33 mg kgdw^{-1}).
(Note: kgdw = kilogram dry weight.)

Selenium concentrations in creek sediments, bank soils, coal ash, and biofilms were close to or exceeded the toxic effect threshold concentration for freshwater sediments (2 mg kgdw^{-1}). The toxic effect threshold is a guideline "for assessing the degree of contamination and relative toxic threat to aquatic life" (Lemly 2002; May et al. 2008). Selenium concentrations in creek sediments showed no distinct pattern along MB and had an average value of 7.1 mg kgdw^{-1}. In bank soils and biofilm samples, Se concentrations decreased from MCK 2.2 to MCK 2, then remained relatively constant (Figure 24).

There are insufficient data to compare As and Se concentrations over time in bank soils, coal ash, benthic biofilms, and creek sediments.

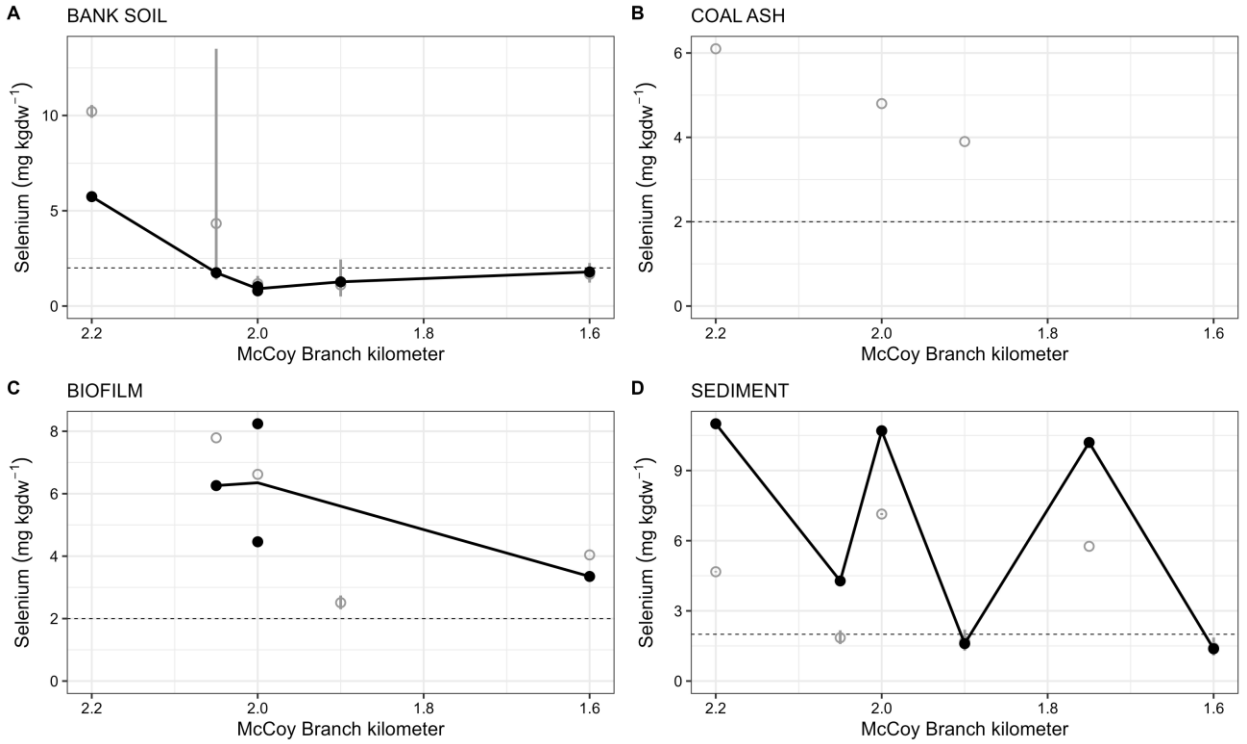

Figure 24. Selenium concentrations along McCoy Branch in (A) bank soils, (B) coal ash in creek banks, (C) benthic biofilms, and (D) creek sediments. Filled symbols represent the results from 2023. Open symbols represent the geometric mean (± standard error) of results from previous years. The horizontal dashed line represents the toxic effect threshold concentration for Se in sediments (2 mg kgdw^{-1}).
(Note: kgdw = kilogram dry weight.)

3.3 BIOTA SAMPLING

3.3.1 Bioaccumulation Results

Average wet weight Se concentrations in largemouth bass fillets collected in RQ in 2023 (0.62 µg/g) again decreased slightly, such that they were the lowest concentrations seen on record (Figure 25). Using percent moisture of fish fillets, the wet weight concentration converts to 3.1 µg/g dry weight, which is below the 11.3 µg/g tissue criterion for Se in fillets (this criterion was adopted by the state of Tennessee in 2019). Concentrations of Se were also measured in ovaries from largemouth bass from RQ. The average wet weight Se concentration in ovaries in 2023 was 1.36 µg/g—lower than concentrations seen in previous years. Using percent moisture for ovaries, the wet weight concentration converts to 3.99 µg/g dry weight, which is below the 15.1 µg/g tissue criterion for Se in ovaries. Concentrations of As in bass fillets from RQ remained low, comparable with previous years. Average wet weight Hg concentrations in largemouth bass fillets increased slightly in 2023 (0.50 µg/g) but remained within the range of concentrations seen in recent years.

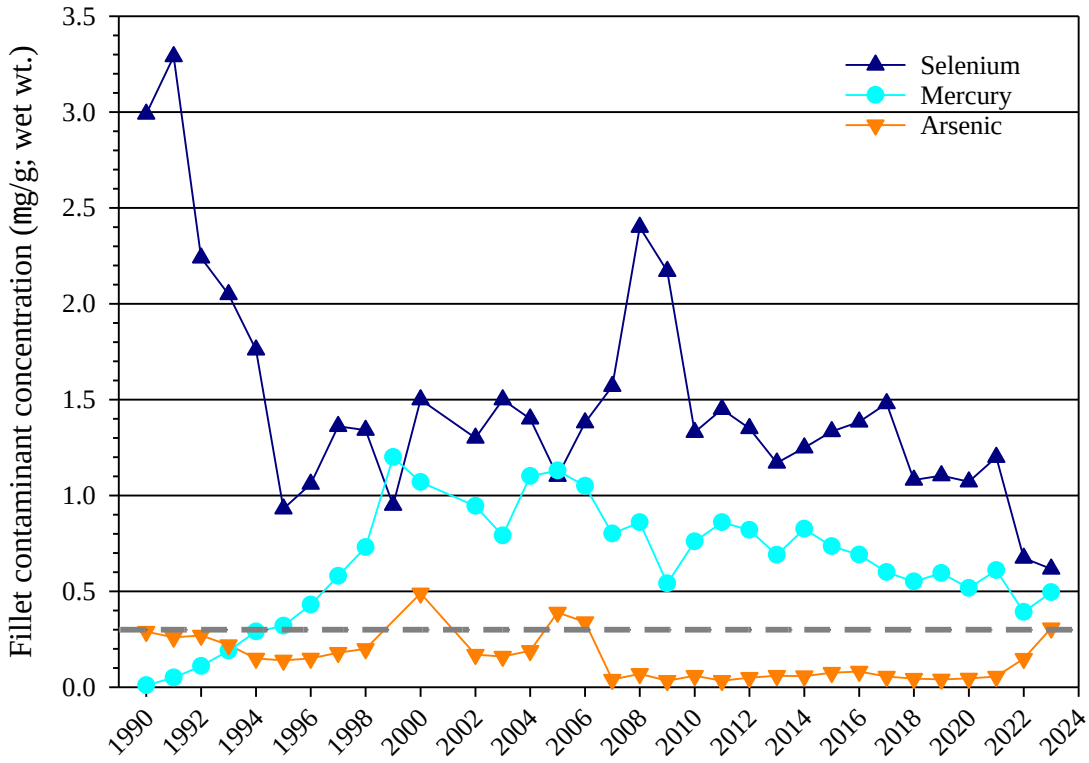

Figure 25. Average wet weight concentrations of Se, Hg, and As in fillets of largemouth bass from Rogers Quarry (1990–2023; *n* = 6 fish/year). The dashed gray line indicates federal recommended ambient water quality criterion for Hg in fish fillets (0.3 µg/g; wet wt.).

Figure 26 shows Se, Hg, and As dry weight concentrations in whole-body forage fish from the watershed. As in 2022, average Se concentrations in whole-body blacknose dace collected in 2023 at MCK 2.0 (10.9 µg/g dry weight) and MCK 1.9 (8.9 µg/g dry weight) remained above federal ambient water quality criterion (AWQC) guidelines (8.5 µg/g dry weight; used as screening level). Previous work has shown elevated aqueous MeHg concentrations below the thermocline within the quarry, suggesting that hypoxic or anoxic conditions at depth in the quarry may create habitats for Hg methylation. Regardless, in 2023, Hg concentrations in forage fish remained low. In 2023, As concentrations in blacknose dace did not decrease with distance downstream but were similar among sites (ranging from 1.47 to 1.55 µg/g dry weight). The As concentrations in fish have decreased significantly over the past few years since wetland maintenance activities were performed in FY 2019, but the Se concentrations in fish have not changed significantly.

Aqueous concentrations of Se were below detection limits in the MB and RQ watershed, but fish tissue concentrations were elevated throughout the watershed and have been at or above the tissue criterion in upper MB in the past few years. Therefore, caged clams were deployed throughout this watershed in FY 2023 to investigate food chain exposure to Se and other coal ash–associated contaminants. Figure 27 shows Se, Hg, and As concentrations in caged clams throughout the watershed. Consistent with point source dilution, Se concentrations were highest in clams deployed in the FCAP wetland and generally decreased with distance downstream in MB and RQ such that concentrations at the downstream sites were comparable with concentrations seen in clams from the reference site. Hg concentrations were highest in clams from the reference site (0.19 µg/g dry weight), which is indicative of overall low Hg concentrations in RQ and MB. While As concentrations were highest in clams deployed at MCK 2.0, concentrations were also elevated in the FCAP wetland, RQ at depth, and lower MB. Concentrations at all other sites

were similar to one another, with a slight decreasing trend with downstream distance from FCAP, but As concentrations throughout the MB and RQ watershed were generally higher than concentrations seen in clams collected from the reference site.

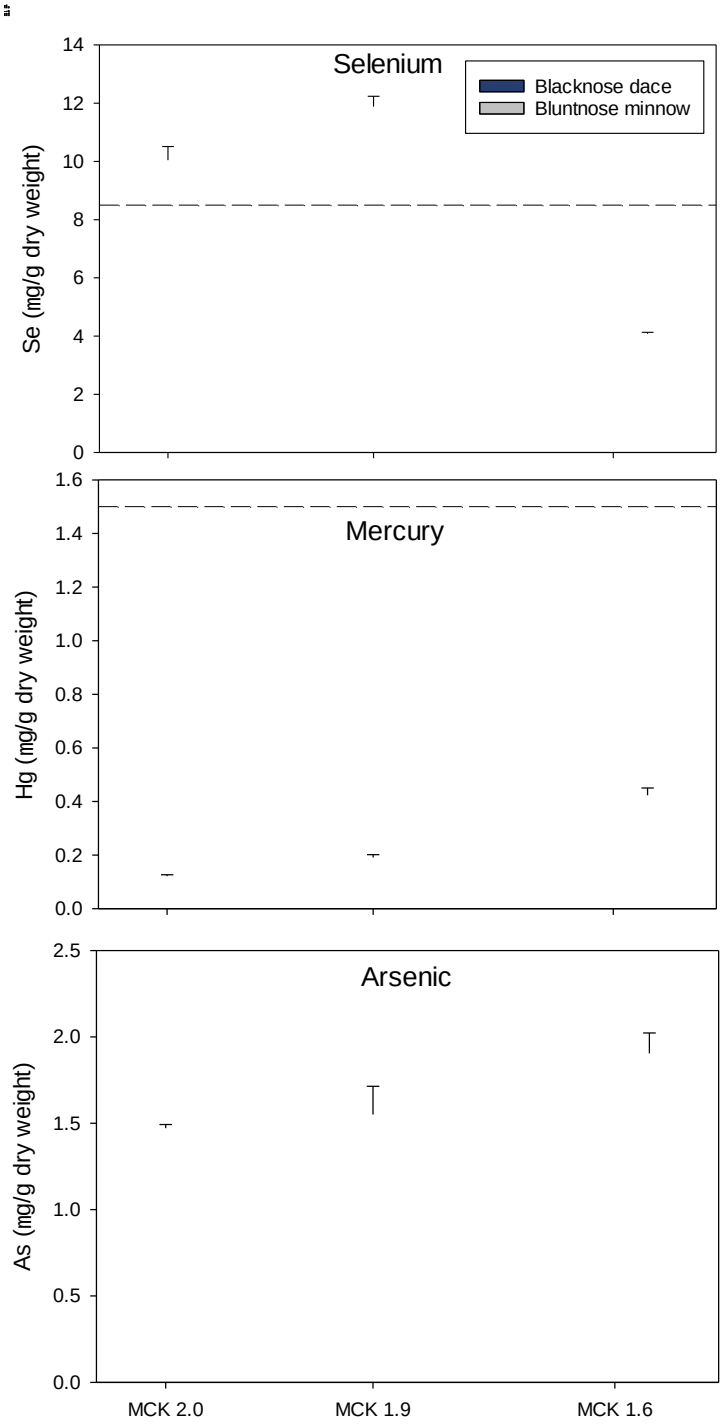

Figure 26. Average dry weight concentrations of Se, Hg, and As in whole-body forage fish from the McCoy Branch watershed, 2023. Dotted black lines indicate federal recommended ambient water quality criterion for Se in whole-body fish (8.5 µg/g dry weight) and for Hg in fish fillets (0.3 µg/g, converted to 1.5 µg/g dry weight). These are screening criteria.

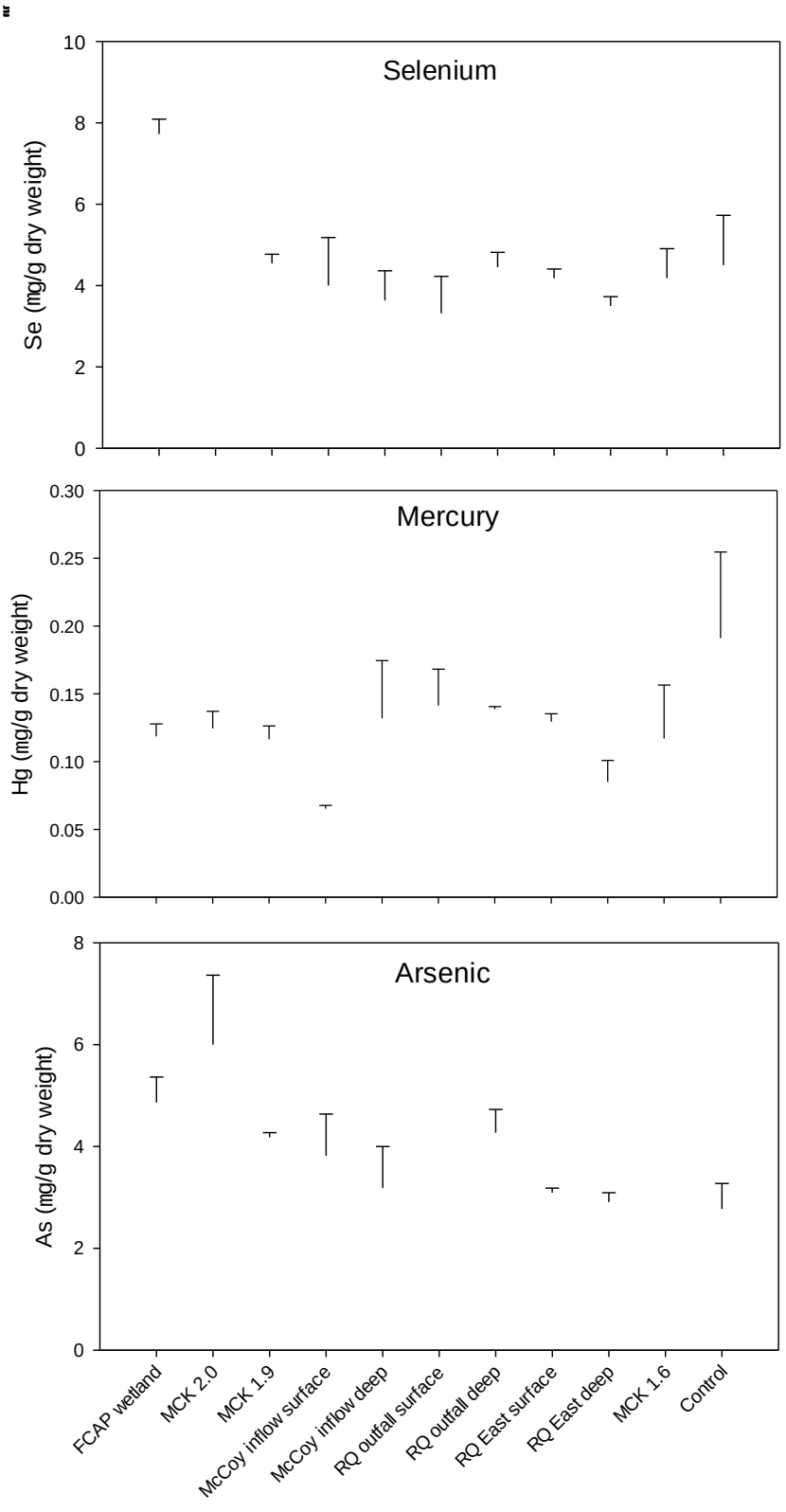

Figure 27. Average wet weight concentrations of Se, Hg, and As in soft tissues of caged Asiatic clams deployed in the McCoy Branch watershed, 2023.

3.3.2 Fish Population Abundance Estimation and Community Survey

Thirty-four largemouth bass were captured in RQ in 2023, the third consecutive year with decreasing captures (Figure 28A). Of these fish, 44% (n = 15) were recaptures of fish marked in previous years, which is the highest percentage since 2019 (Figure 28B). It should be noted that fewer anglers participated in sampling in 2023 (n = 2 versus n = 3 in previous years), which may have contributed to the lower number of captured bass.

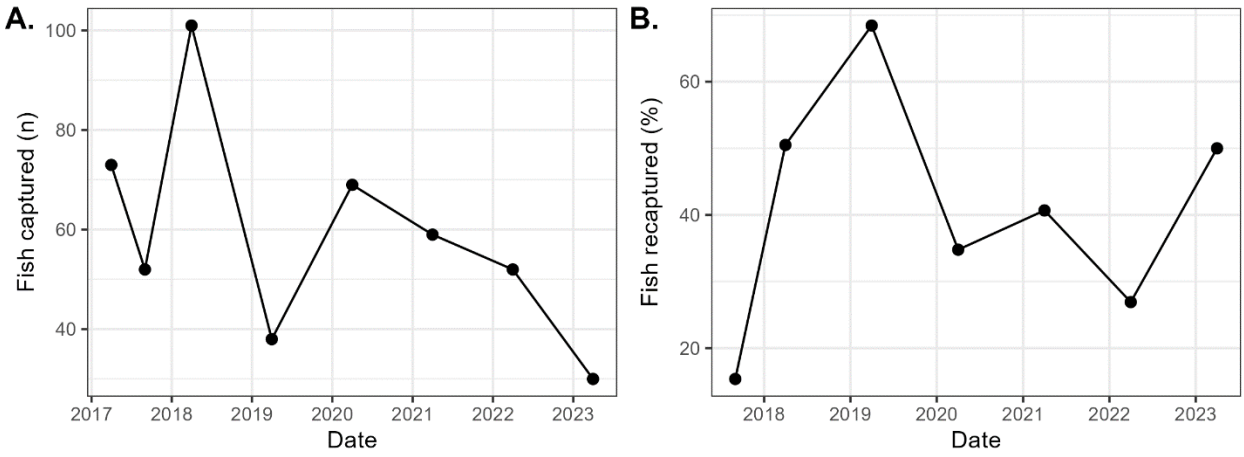

Figure 28. Temporal patterns in (A) largemouth bass captured during surveys in Rogers Quarry and (B) the percentage of captured fish that had been previously tagged. Note that recaptures were only possible following the initial survey, so there is no data point for April 2017 in (B).

Of the eight POPAN models that were run, the model that included recapture probability (p) and probability of entry into the population (p_{ent}) as time-varying parameters was the best fit to the capture history data (Table 3). However, because of the low number of fish captured in 2023, this model was unable to estimate confidence intervals for these parameters. Alternatively, if we assume that capture probability (p) remains constant while apparent survival (ϕ) and entry into the population (p_{ent}) vary through time, the estimated largemouth bass population (estimate ± 95% confidence interval) in RQ in 2023 was 94 ± 38 fish, indicating a decline in population size since 2020 (Figure 29). In terms of parameters, the model estimated that capture probability (p) was 0.351 ± 0.072 and superpopulation size was 591 ± 96, both of which were held constant across years. Apparent survival (ϕ) ranged from 0.379 ± 0.220 to 1.000 ± 0.000, and the probability of entry into the population (p_{ent}) ranged from 0.018 ± 0.051 to 0.132 ± 0.067 across the years (Table 4). Taken as a whole, these results suggest that the largemouth bass population in RQ may be declining over the time of this study, with the estimated population in 2023 being approximately half the size of the population as estimated for 2020. The selected model suggests that the annual variability in population size is driven by reduced recruitment into the population (estimates of p_{ent} through time) as opposed to changes in apparent survival (estimates of ϕ through time). However, current sampling methods (angling) may be biased toward larger fish and unable to accurately estimate the abundance of smaller sized fish (< 30 cm). Further targeted study would be required to specifically address these drivers.

Table 3. Results for selection of best-fit POPAN model. Parameters either were held constant through time (.) or were allowed to vary across time intervals (*t*). Best-fit model identified based on lowest AIC_c score

Model	Number of parameters	AIC_c	ΔAIC_c	Weight	Deviance
$\phi(.)\ p(t)\ p_{ent}(t)\ N(.)$	17	794.5	0.0	0.591	-1144.1
$\phi(.)\ p(t)\ p_{ent}(.)\ N(.)$	11	795.3	0.8	0.401	-1130.4
$\phi(.)\ p(.)\ p_{ent}(t)\ N(.)$	10	804.3	9.7	0.005	-1119.4
$\phi(t)\ p(t)\ p_{ent}(t)\ N(.)$	23	805.9	11.4	0.002	-1145.9
$\phi(t)\ p(.)\ p_{ent}(t)\ N(.)$	16	807.1	12.6	0.001	-1129.3
$\phi(t)\ p(t)\ p_{ent}(.)\ N(.)$	17	809.5	15.0	0.000	-1129.1
$\phi(t)\ p(.)\ p_{ent}(.)\ N(.)$	10	810.9	16.4	0.000	-1112.7
$\phi(.)\ p(.)\ p_{ent}(.)\ N(.)$	4	820.5	26.0	0.000	-1090.7

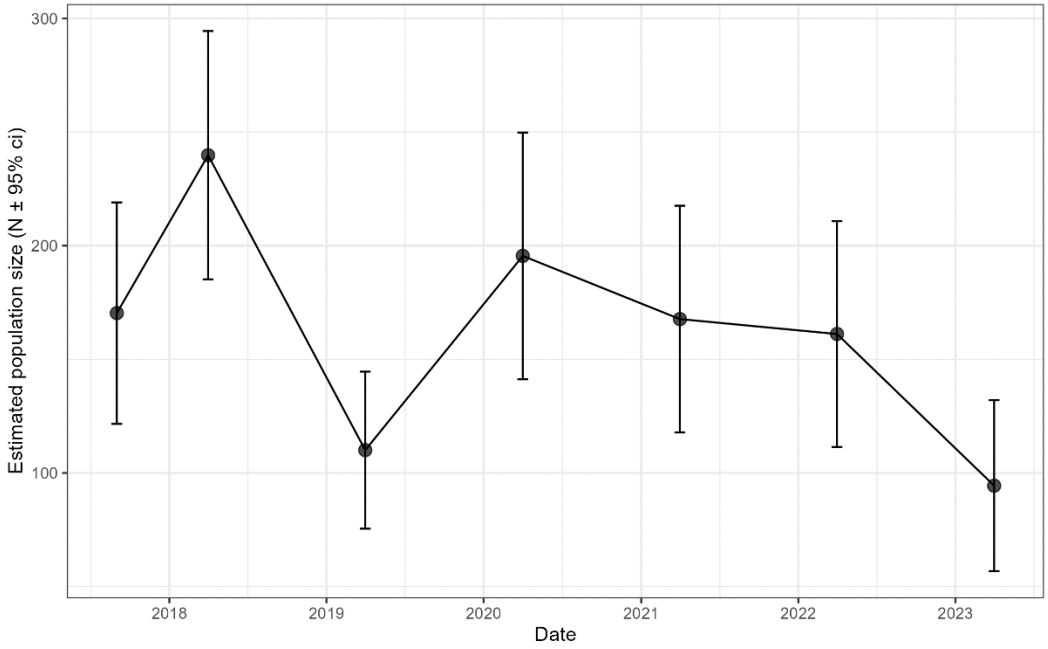

Figure 29. Time series of POPAN estimate (±95% confidence interval [ci]) of largemouth bass population size in Rogers Quarry during the study period.

Table 4. POPAN population parameters for ϕ and p_{ent} estimated for each time interval from best-fit model of largemouth bass in Rogers Quarry. Parameters (estimate ±95% confidence interval [ci]) for capture probability (0.351 ± 0.072) and superpopulation size (591 ± 96) were held constant through time

Survey date	ϕ (estimate ±95% ci)	p_{ent} (estimate ±95% ci)
April 2017	0.379 ± 0.220	—
September 2017	1.000 ± 0.000	0.072 ± 0.083
April 2018	0.414 ± 0.137	0.117 ± 0.077
April 2019	0.878 ± 0.318	0.018 ± 0.051
April 2020	0.504 ± 0.199	0.167 ± 0.068
April 2021	0.494 ± 0.228	0.117 ± 0.067
April 2022	0.495 ± 0.270	0.132 ± 0.067
April 2023	—	0.025 ± 0.056

3.3.3 Fish Health

No deformed or emaciated largemouth bass or other fish were detected in RQ in 2023 (Table 5). Length frequency histograms show that fish collected in 2023 were similar to fish collected in 2022, though potential cohorts were more difficult to distinguish (Figure 30). The median value estimated for Fulton's condition factor (*K*) decreased in 2023 from a maximum observed in 2022 but is still higher than in previous years (Figure 31). Closer inspection shows that this decrease was likely due in large part to four smaller fish (≤ 30 cm) that were in poor condition (K < 1), which had not been observed since 2020 (Figure 31). Taken together, these data suggest that fish health in RQ may differ between older (larger) and younger (smaller) fish, which may be contributing to the decreased population sizes reported in Section 3.3.2.

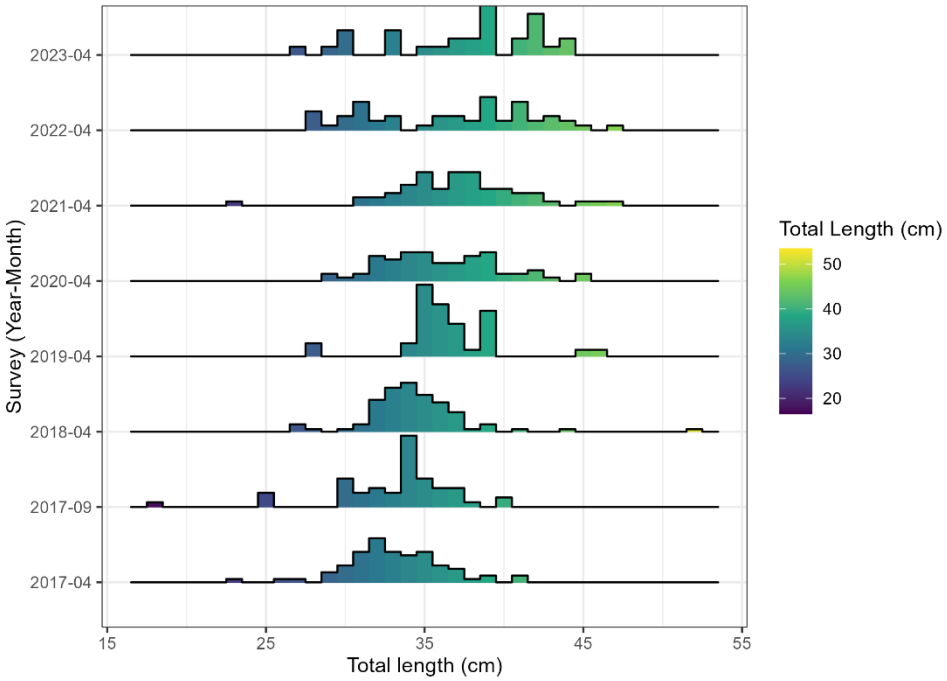

Figure 30. Ridgeline plot showing length distributions of largemouth bass collected at Rogers Quarry from 2017 to 2023.

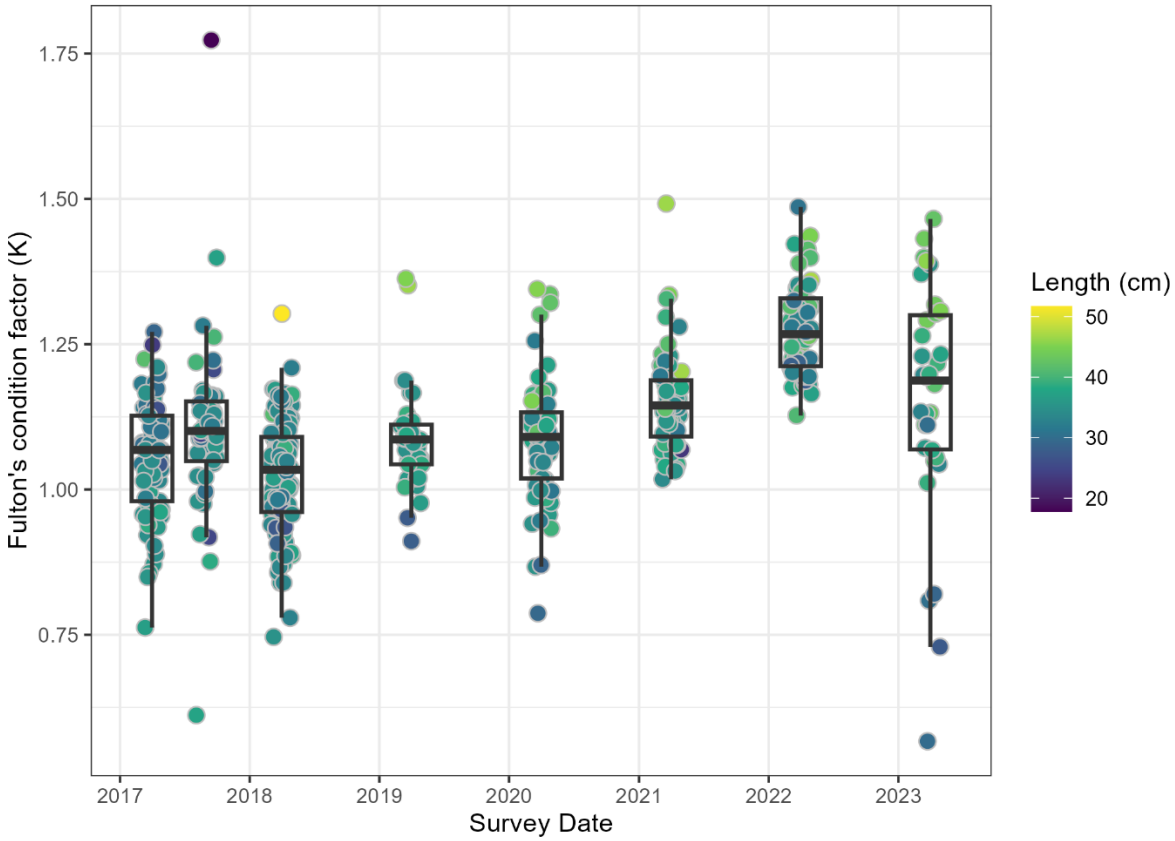

Figure 31. Distribution in *K* for all largemouth bass captured in Rogers Quarry from 2017 to 2023. Each point represents a single fish captured, and the total length of each fish is indicated by fill color.

Table 5. Average ± standard error for meristic measurements from deformed (2017 only) and normal largemouth bass collected in Rogers Quarry (2017–2023)

Metric	Rogers 2017 deformed (*N* = 6)	Rogers 2017 normal (*N* = 8)	Rogers 2018 (*N* = 10)	Rogers 2019 (*N* = 6)	Rogers 2020 (*N* = 7)	Rogers 2021 (*N* = 8)	Rogers 2022 (*N* = 6)	Rogers 2023 (*N* = 6)
Standard length (SL; cm)	29.19 ± 0.81	33.55 ± 1.73	31.32 ± 1.25	34.24 ± 1.22	33.88 ± 0.69	34.09 ± 1.24	33.47 ± 4.36	37.31 ± 3.54
Total length (cm)	34.42 ± 0.92	39.28 ± 2.04	36.94 ± 1.54	36.62 ± 1.19	39.28 ± 0.73	37.21 ± 0.51	38.44 ± 5.47	42.1 ± 3.93
Head length (HL; cm)	9.14 ± 0.57	10.74 ± 0.69	9.42 ± 0.40	11.13 ± 0.32	11.05 ± 0.22	11.26 ± 0.48	10.15 ± 1.42	11.56 ± 1.01
Eye diameter (ED; cm)	1.20 ± 0.08	1.37 ± 0.09	1.28 ± 0.08	1.40 ± 0.05	1.48 ± 0.04	1.28 ± 0.09	1.22 ± 0.2	1.53 ± 0.12
Preorbital length (PrOL; cm)	3.62 ± 0.23	3.17 ± 0.31	3.56 ± 0.18	2.19 ± 0.12	2.23 ± 0.07	2.73 ± 0.17	2.06 ± 0.36	2.3 ± 0.25
Postorbital length (PosOL; cm)	5.72 ± 0.36	7.25 ± 0.50	6.23 ± 0.43	7.55 ± 0.27	7.41 ± 0.17	7.64 ± 0.35	6.95 ± 0.96	7.99 ± 0.91
Predorsal distance (PrDD; cm)	11.31 ± 11.31	13.83 ± 0.88	11.90 ± 0.54	13.41 ± 0.84	13.69 ± 0.44	14.61 ± 0.60	13.21 ± 2.05	15.04 ± 1.5
Prepectoral distance (PrPD; cm)	9.47 ± 0.71	11.12 ± 1.03	9.32 ± 0.44	12.20 ± 0.37	11.52 ± 0.29	12.91 ± 0.57	11.57 ± 1.72	13.08 ± 1.3
Preventral distance (cm)	10.34 ± 0.56	12.12 ± 0.82	10.64 ± 0.52	12.71 ± 0.48	12.50 ± 0.29	12.95 ± 0.23	11.82 ± 1.73	13.89 ± 1.18
Preanal distance (cm)	18.38 ± 0.67	22.12 ± 1.35	19.11 ± 0.86	22.74 ± 0.89	22.88 ± 0.51	23.00 ± 0.81	22.36 ± 3.08	22.71 ± 2.29
Dorsal fin length (cm)	10.38 ± 0.49	10.95 ± 0.78	10.49 ± 0.47	13.98 ± 0.62	13.75 ± 0.35	14.30 ± 0.56	13.47 ± 1.43	15.17 ± 1.31
Caudal peduncle length (cm)	4.83 ± 0.45	5.97 ± 0.35	5.34 ± 0.26	7.04 ± 0.30	6.87 ± 0.17	6.67 ± 0.58	7.46 ± 1.78	8.24 ± 1.08
Anal peduncle length (cm)	4.43 ± 0.15	5.94 ± 0.33	4.80 ± 0.19	6.15 ± 0.25	6.26 ± 0.15	6.94 ± 0.17	7.11 ± 1.35	7.99 ± 0.82
Caudal fin length (cm)	5.23 ± 0.17	5.72 ± 0.33	5.62 ± 0.34	6.95 ± 0.21	6.81 ± 0.15	6.76 ± 0.35	5.68 ± 1.29	7.45 ± 0.75
Anal fin length (cm)	3.31 ± 0.15	3.91 ± 0.37	4.10 ± 0.20	5.50 ± 0.28	5.25 ± 0.17	5.25 ± 0.35	4.76 ± 0.38	5.97 ± 0.65
Pectoral–ventral length (cm)	2.69 ± 0.12	3.28 ± 0.21	3.30 ± 0.19	4.13 ± 0.22	4.20 ± 0.13	4.59 ± 0.22	4.19 ± 0.6	5.14 ± 0.56
Ventral–anal length (cm)	8.46 ± 0.30	10.88 ± 0.69	9.08 ± 0.39	10.25 ± 0.56	10.96 ± 0.35	10.38 ± 0.59	10.91 ± 2.33	10.41 ± 1.29
Pectoral fin length (cm)	4.59 ± 0.39	6.16 ± 0.44	5.24 ± 0.28	6.00 ± 0.15	6.19 ± 0.12	6.23 ± 0.28	6.22 ± 0.78	7.04 ± 0.82
Ventral fin length (cm)	3.70 ± 0.24	3.95 ± 0.38	3.89 ± 0.14	2.03 ± 0.14	1.67 ± 0.11	4.93 ± 0.25	4.97 ± 0.71	5.07 ± 0.39
Body depth (cm)	6.95 ± 0.25	8.97 ± 0.65	7.69 ± 0.36	10.28 ± 0.53	10.35 ± 0.31	11.21 ± 0.67	10.19 ± 1.49	11.57 ± 1.18
Body least depth (cm)	2.77 ± 0.09	3.51 ± 0.27	2.94 ± 0.13	3.96 ± 0.16	3.58 ± 0.10	4.30 ± 0.26	3.67 ± 0.54	4.29 ± 0.48
HL:SL (NU*)	0.31 ± 0.01	0.32 ± 0.01	0.30 ± 0.00	0.33 ± 0.01	0.33 ± 0.00	0.33 ± 0.01	0.30 ± 0.01	0.31 ± 0.01
PrOL:SL (NU*)	0.12 ± 0.01	0.10 ± 0.01	0.30 ± 0.00	0.06 ± 0.00	0.07 ± 0.00	0.08 ± 0.01	0.06 ± 0.01	0.06 ± 0.01
PosOL:SL (NU*)	0.20 ± 0.01	0.22 ± 0.01	0.20 ± 0.20	0.22 ± 0.02	0.22 ± 0.00	0.22 ± 0.00	0.21 ± 0.01	0.21 ± 0.01
PrPD:SL (NU*)	0.32 ± 0.01	0.33 ± 0.02	0.30 ± 0.00	0.36 ± 0.01	0.34 ± 0.00	0.38 ± 0.01	0.35 ± 0.01	0.35 ± 0.01
PrDD:SL (NU*)	0.39 ± 0.81	0.41 ± 0.01	0.38 ± 0.00	0.39 ± 0.02	0.40 ± 0.01	0.43 ± 0.03	0.39 ± 0.01	0.4 ± 0.01
ED:HL (NU*)	0.13 ± 0.01	0.04 ± 0.00	0.14 ± 0.01	0.13 ± 0.00	0.13 ± 0.00	0.11 ± 0.02	0.12 ± 0.01	0.13 ± 0.01
PrOL:HL (NU*)	0.40 ± 0.01	0.30 ± 0.03	0.38 ± 0.00	0.20 ± 0.01	0.20 ± 0.01	0.24 ± 0.01	0.20 ± 0.02	0.2 ± 0.02
PosOL:HL (NU*)	0.63 ± 0.02	0.67 ± 0.01	0.66 ± 0.02	0.68 ± 0.01	0.67 ± 0.01	0.68 ± 0.02	0.69 ± 0.03	0.69 ± 0.03

Note: The columns give the average ± standard error for all fish collected from 2017 to 2023.
*NU = unitless metric.

4. SUMMARY

4.1 WATER QUALITY AND SOLIDS SAMPLING

Total Hg and total dissolved Hg concentrations in water samples collected in 2023 throughout the MB and RQ system were significantly higher than concentrations measured in previous years. We cannot narrow down when the concentrations began to increase during the 11 months preceding sample collection. We advocate for an increased sampling frequency providing better temporal resolution to understand future concentration changes, or lack thereof, as well as any future consequent effects of higher inorganic Hg concentration on MeHg concentration.

With respect to the remaining parameters, surface water samples in the MB and RQ system were generally unremarkable with the exception of As concentrations at MCK 2.05, which exceeded the EPA drinking water standard. Total and dissolved Se concentrations were highest at MCKs 2.05 and 2.0, but all samples remained below the EPA aquatic life water quality criterion. Water quality monitoring from the FCAP and along MB should continue to verify the absence of breakthrough from MCK 2.05 to locations downstream.

Vertical profiling within RQ shows a thermally stratified water body. DO concentrations fell below the detection limit at the deepest locations. The anoxic conditions below the thermocline create conditions favorable for Hg methylation, consistent with high MeHg concentrations in the deepest samples, and for reduced forms of As (arsenite; As[III]) and Se (selenite; Se[-II]) to dominate speciation of these elements. The implications for the predominance of reduced forms of As and Se are important because arsenite is three to five times more toxic than arsenate, and selenite is more toxic than selenate in aquatic ecosystems.

Creek solids (i.e., sediments, bank soils, coal ash, biofilm) had high concentrations of both As and Se. Most samples had measured concentrations that exceeded or were close to the respective consensus adverse effect limits, including sediments collected from the bottom of RQ.

In addition to the need for increased sampling frequency to better understand changes in Hg concentrations, future studies should target improved characterization and quantification of biogeochemistry through the water column and in the sediments of RQ both spatially and temporally. For example, to date, annual sampling occurs on a single day with profiling and sample collection at one location within the quarry. The longer-term temperature monitoring collected in 2017–2018 demonstrated substantial vertical changes (at one location) over time. To better understand the spatial distribution of conditions and water quality, these samplings should be conducted at multiple locations numerous times throughout the year. Additionally, the 2017–2018 temperature record suggests that turnover is possible, which would deliver high MeHg- and As-containing water to the surface of RQ and potentially to MB downstream of the quarry. Confirmatory sampling campaigns should be designed and conducted to assess this potential exposure pathway.

4.2 BIOTIC SAMPLING

Monitoring of forage fish throughout MB continues to show Se concentrations that are above federal AWQC for whole-body fish in upper MB, despite actions taken in the FCAP wetland. However, Se concentrations in both forage fish and caged clams deployed throughout MB decreased rapidly with distance downstream. Selenium concentrations in largemouth bass collected from RQ were the lowest on record at this site. Field observations of fish and meristic measurements made in 2023 did not suggest abnormalities in the RQ largemouth bass. Results from the mark-recapture study suggest that the largemouth bass population may be decreasing because of reduced entry of younger (smaller fish) into the

population. Length and weight data indicate that the relative conditions of larger (older) fish have improved, but the conditions of these smaller fish declined in 2023 for reasons as yet unknown. However, as more data are collected, the increasingly comprehensive picture of the RQ ecosystem may elucidate patterns in environmental conditions that are linked to increased Se burdens in fish, fish deformities, or other effects pointing to the benefits of continuing to monitor this ecosystem.

5. REFERENCES

EPA (US Environmental Protection Agency). 1996. *Determination of Trace Elements in Ambient Waters by Inductively Coupled Plasma–Mass Spectrometry*. EPA Method 1638, Office of Water, Washington, DC. http://www.caslab.com/EPA-Methods/PDF/EPA-Method-1638.pdf.

Laake, J. 2013. *RMark: An R Interface for Analysis of Capture-Recapture Data with MARK*. AFSC Processed Rep. 2013-01, Alaska Fisheries Science Center, National Oceanic and Atmospheric Administration, National Marine Fisheries Service, Seattle, Washington.

Lemly, A. D. 2002. "Interpreting Selenium Concentrations." In *Selenium Assessment in Aquatic Ecosystems: A Guide for Hazard Evaluation and Water Quality Criteria* 18–38. New York: Springer.

MacDonald, D. D., C. G. Ingersoll, and T. A. Berger. 2000. "Development and Evaluation of Consensus-Based Sediment Quality Guidelines for Freshwater Ecosystems." *Archives of Environmental Contamination and Toxicology* 39 (1): 20–31.

May, T. W., J. F. Fairchild, J. D. Petty, M. J. Walther, J. Lucero, M. Delvaux, J. Manring, and M. Armbruster. 2008. "An Evaluation of Selenium Concentrations in Water, Sediment, Invertebrates, and Fish from the Solomon River Basin." *Environmental Monitoring and Assessment* 137: 213–232.

Perea, S., J. Vukić, R. Šanda, and I. Doadrio. 2016. "Ancient Mitochondrial Capture as Factor Promoting Mitonuclear Discordance in Freshwater Fishes: A Case Study in the Genus Squalius (Actinopterygii, Cyprinidae) in Greece." *PLOS ONE* 11 (12): e0166292.

R Core Team. 2023. *R: A Language and Environment for Statistical Computing.* R Foundation for Statistical Computing, Vienna, Austria.

Schwarz, C. J., and A. N. Arnason. 1996. "A General Methodology for the Analysis of Capture-Recapture Experiments in Open Populations." *Biometrics* 52: 860–873.